Mapping varied mental representations: The case of representing illegalized immigrants

Joel E. Martinez[1,2] & Alexander Todorov[3]

[1] Data Science Initiative, Harvard University, Cambridge, MA, USA

[2] Department of Psychology, Harvard University, Cambridge, MA, USA

[2] Booth School of Business, University of Chicago, Chicago, IL, USA

Note: This manuscript has been accepted and is in press at Social Cognition

Abstract

Average images are often estimated within a sample or theory-derived variables (e.g., conservatives vs. liberals) to understand how social categories are mentally represented. However, average representations can mask large internal heterogeneity, thereby missing unexpected or complex representational clustering. We propose an inverted data-driven approach that first clusters representations by similarity, then identifies variables that differentiate clusters. We apply this approach to characterize mental representations of illegalized immigrants. Representations were collected in Texas and California (N=1002) using face-based reverse correlation along with variables theorized to influence perceptions of immigrants: attitudes, demographics, ideologies, geography, and a label manipulation (i.e., "undocumented" vs "illegal" immigrant). Sample- and variable- aggregated images hid representational clusters that differed on visualized facial phenotype and affective expressions. Clustered representations ranged from highly shared to smaller clusters differentiated by demography and social geography: age and local population size perceptions. Data-driven approaches can help reveal meaningful variation in visual representations.

Keywords: Heterogeneity, Illegalized immigrants, Face Representations, Reverse Correlation, Machine Learning

Face-based reverse correlation studies attempt to visualize the mental representations people hold of various social categories (Brinkman et al., 2017; Dotsch et al., 2008; Dotsch & Todorov, 2012; Hinzman & Maddox, 2017; Imhoff et al., 2011; Krosch & Amodio, 2014; Lei & Bodenhausen, 2017). Inferences about who holds which representations are typically made from average classification images that aggregate individual-level representations across the sample or within individual differences variables theorized as important for shaping mental representations. However, relying solely on these averages can lead to misleading inferences about shared beliefs when they mask large underlying variation (Fisher et al., 2018; Martinez et al., 2020; Martinez & Paluck, 2020). Large hidden variation is a sign that theory-derived guesses about variables that differentiate mental representations may not capture the actual partitioning of representations across people. We therefore aim to develop an alternative data-driven analytic approach for quantifying and characterizing representational variation in visual representations: what varied understandings exist for a target category and how are they patterned across people?

We focus on the category of illegalized immigrants whose perceptions are understudied despite urgent political salience. Visual mental representations of illegalized immigrants seem to predominantly depict darker-skinned and threatening faces (Martinez, Oh, et al., 2021a), although disaggregating by nationality and economic status reveals illegality is not always coded as darker skin tones (Martinez, Oh, et al., 2021b). In line with emerging findings that many social judgments are more idiosyncratic than shared across people (Hönekopp, 2006; Kahneman et al., 2021; Martinez et al., 2020), these studies suggest there exists meaningful yet unexamined variation in mental representations of illegalized immigrants.

Approaches to assessing representational variation

Theory-driven approach. While reverse correlation uses a data-driven process in the creation of classification face images, theory-derived variables are commonly used to partition the sample to examine representational differences (e.g., Dotsch et al., 2008; Lei & Bodenhausen, 2017; Young et al., 2014). For instance, political orientation may be identified as an important source of variation based on past research. Average classification images are created separately for liberal and conservative participants and compared. Any differences between the two images could elicit differential evaluations from naïve raters (DeBruine, 2020), which is then interpreted as evidence that different political orientations cluster representations differently.

Although convenient, these theory-driven practices rest on shaky assumptions. First, using categories as units of analysis often fails to capture the social contours of shared beliefs given that within-category disagreements can often be larger than between-category disagreements (Cikara, 2021; Hanel et al., 2019; Martinez & Paluck, 2020). Second, it assumes psychological phenomena are sufficiently summarized and simultaneously determined by multiple independent and powerful main effects, even though this is highly improbable (Tosh et al., 2020). Attempts to find multiple important main effects from an infinite variable space can be very costly in reverse correlation paradigms where average faces must be produced, rated, and compared for each examined variable. Representational variation is instead more likely to arise from complex interactions between dynamic forces and dynamic people (Cikara, Martinez, et al., 2022; Tucker, 2012), creating complex representational clusters that cannot be characterized univariately. The theory-driven practices above amount to predetermined univariate guesses about the sources of representational variation, which can impede examination of unexpected or complex representational clusters.

Inverted data-driven approach. Our approach attempts to bypass the univariate assumptions behind simple aggregation by focusing on quantifying the structure of inter-individual similarity in representations. Correlating across people is not a new idea (Stephenson, 1935) and has been used to identify how socially contested concepts may be understood in varied ways across clusters of participants (Boutyline, 2017; Watts & Stenner, 2005). What *is* new is the development of machine learning techniques that lessen previous computational barriers and loosen restrictive assumptions imposed by confirmatory methods (Breiman, 2001b; Jones & Linder, 2015). The basic proposal is to invert the typical analysis: first identify how people are clustered by the similarity of their representations, *then* describe the extent to which theory-derived variables differentiate between clusters to help interpret them. Our approach therefore combines both data-driven and theory-driven insights to reveal important and hidden patterns from reverse correlation data.

The analytic pipeline developed for this study occurs in four steps followed by a validation procedure (**Figure 1**). First, compute individual-level representations (i.e., the selected noise pattern before it is overlaid on the base face). Second, correlate individual representations with each other to create a participant x participant similarity matrix. Third, use a clustering algorithm to identify structure in the similarity matrix, clusters of people who visualized similar faces. Lastly, compute average classification images for each cluster to summarize representations within each cluster. Many of the steps require researchers to make multiple important analytic decisions despite the data-driven spirit of this pipeline (see methods).

This approach attempts to strike a balance between competing conceptualizations of the relationship between individual and average classification images. One perspective sees the individual images as noisy and averaging as a process that extracts meaningful signal (Brinkman et al., 2017), while the other sees the individual images as a better reflection of existing representational variation while averages neglect to account for that variation (Cone et al., 2020). The former is limited by problems with sample averages being non-representative while the latter is limited by costs associated with analyzing large collections of individual images and that some aggregation of information across people is eventually needed since shared beliefs cannot be quantified solely from individual representations. In our proposal, averages created from first clustering people with similar representations should be more representative of the averaged participants than previously used averaging approaches (e.g., full sample averages, sample-bootstrapped averages, or variable-derived averages).

A potential issue with our approach is that cluster algorithms may find clusters even within random noise, so adding validation procedures can help identify whether *meaningful* clusters have been found. We focus on two checks: 1) how the average cluster images are evaluated along various traits to help characterize the content that differentiates clusters and 2) whether theory-derived variables track differences in cluster membership as would be expected. Meaningful clusters can be said to be found to the extent that the individual differences match representational content in a theoretically consistent manner. To map variables to cluster memberships, we take advantage of fairly recent advances in machine learning classification models: decision trees (Hothorn et al., 2006) and random forests aggregate and summarize many decision trees (Breiman, 2001a). These combined approaches are promising for this application for the following reasons: decision trees can uncover complex interactions between variables and cluster membership in line with the idea that psychological phenomena are shaped by complex influences; random forests provide a robust way to cross-validate the important variables found in the decision tree; and innovations in interpretable machine learning have opened up the "black box" of random forests to help characterize the relationships between variables and cluster memberships that the model learns (Molnar, 2020).

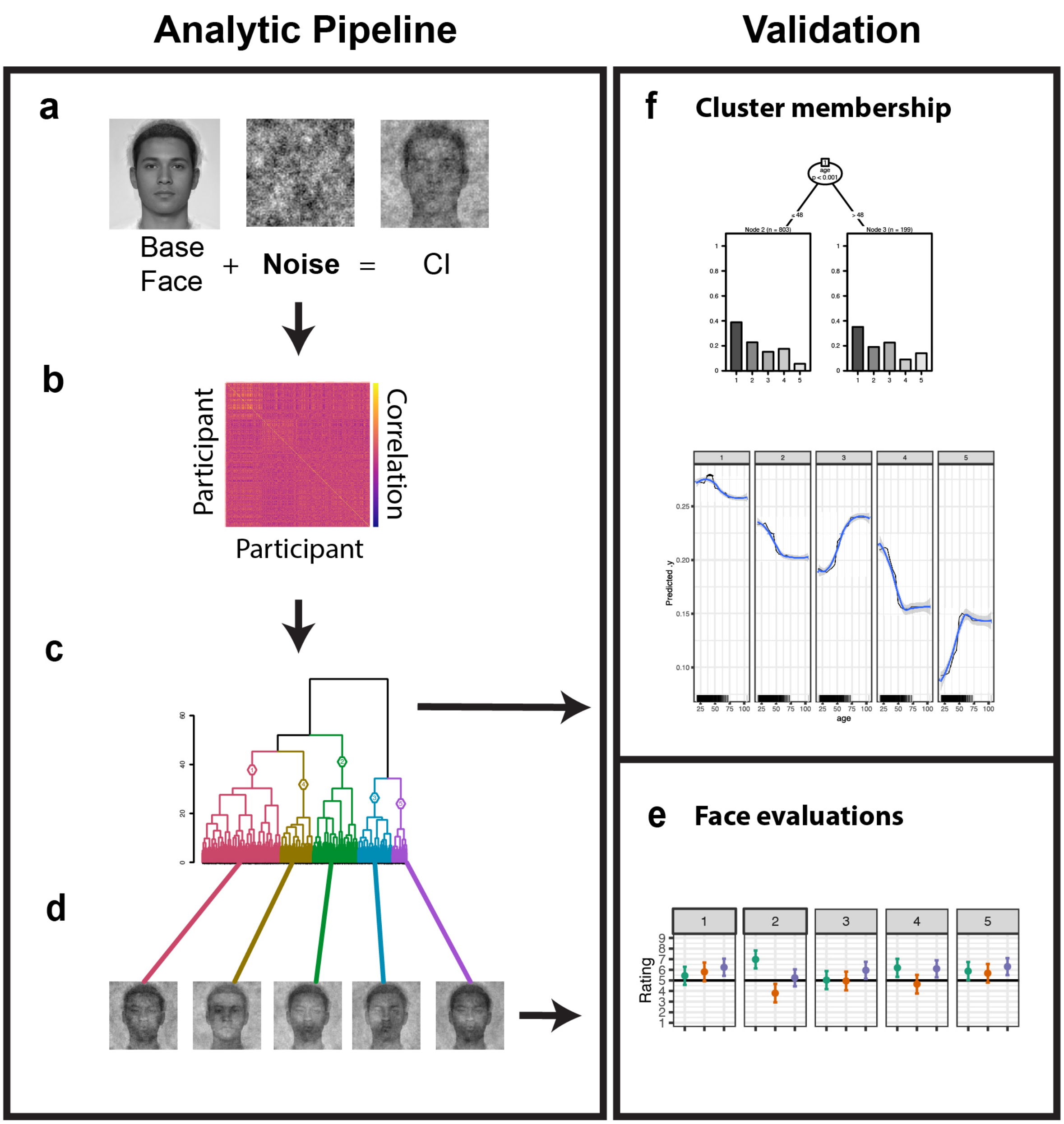

Figure 1. Analytic pipeline and validation procedures. The analytic pipeline consists of four steps: **a.** collect all the participants' individual noise representations, **b.** correlate the individual representations to create a participant x participant similarity matrix, **c.** find clusters using a hierarchical clustering algorithm, and **d.** compute an average face for each cluster. The validation pipeline consists of two main analyses to validate the choice of clusters: **e.** investigate whether evaluations of the average faces differ in ways that conceptually match the associated individual differences for each cluster and **f.** find individual difference measures that can predict cluster membership (top panel is a decision tree, bottom panel is variable-cluster mappings from a random forest).

Current study

The goal of this study is to develop a more comprehensive analytic framework for quantifying visual mental representations of social categories, with illegalized immigrants as a case study. Our proposed data-driven approach should reveal varied visual understandings of the category “undocumented immigrant”. First, we show the problems that arise when attempting to understand this question using a theory-driven averaging approach. We then apply the proposed data-driven pipeline to the classification images, showcasing its advantages. Evaluations of the content of the clustered representations occurred through dangerous, American, and ethnoracial classifications, shown to be important for representations of immigrants (Martinez, Oh, et al., 2021a, 2021b). We additionally included dominance, which is considered a fundamental dimension of face perception (Todorov & Oosterhof, 2011).

Cluster membership was characterized using variables theorized to be important in shaping perceptions of immigrants. These influences originate from a) attitudes (Ommundsen et al., 2014), b) demographics like education level or religious affiliation (Abrajano & Hajnal, 2015; Davis & Perry, 2020), c) political ideologies or party affiliations (Chavez, 2013; Kunst et al., 2019; Sati, 2020; Sides et al., 2018), d) social geography like state or local environments and population size perceptions (Cikara, Fouka, et al., 2022; Craig & Richeson, 2018; Huo et al., 2018b, 2018a), and e) linguistic labels like “undocumented” vs “illegal” immigrant (Ackerman, 2013; Plascencia, 2009; Rosa, 2019; Rucker et al., 2019). While attitude, demographic, and ideological variables can easily be measured within the task, assessing contributions from geographic and label variables requires explicitly accounting for them in the experimental design. Therefore, we focused on collecting representations from California and Texas, two states on the Mexico-U.S. border. Within each state, we asked half of the participants to visualize “undocumented immigrants” and the other half “illegal immigrants”.

These design choices were considered carefully for they are related. Both Texas and California are border states, have large overall populations, and each have a population of over 400,000 illegalized immigrants (Pew Research Center, 2019b). However, they differ in the dominant sentiment of their political institutions and discourses towards immigrants. Texas had no sanctuary cities at the time of this study and “illegal immigrant” was a more common search term on Google from its residents, while California had many sanctuary cities and its residents tended to search more for “undocumented immigrant” (Griffith, 2021) (see **Supplementary Figure S1**). This connection between place and language even occurs at the level of state legislation where California bills tend to use “undocumented” labeling while conservative states like Arizona mainly use “illegal” language in their legislation (Filindra & Kovács, 2012). Given that institutional signals of inclusion or exclusion serve as social norm cues (Tankard & Paluck, 2016), state-level political culture may become symbolically ingrained as a normative community value or accessible schema that shapes its residents’ representations of illegalized immigrants (Huo et al., 2018a, 2018b; Zaller, 1992). However, there is also considerable within-state variation in immigrant policy, sentiment, presence, and contact (Varsanyi et al., 2012), which could influence local demographic perceptions independent of state-level factors (Enos, 2017). These states are therefore useful cases for attempting to capture representational variation from labels and geographic differences at various geographic levels.

Methods

The data and analysis scripts are archived on the Open Science Framework: https://osf.io/z32fn/. The project was approved by the Princeton University IRB #7301. This study was not preregistered. We report how we determined our sample size, all manipulations, and all measures in the study.

Image generation task

Participants

Participants were sampled from Amazon Mechanical Turk in December 2019, with settings that restricted access to the task solely to participants who lived in California (N = 500) or Texas (N = 502). Half of the participants in each state either visualized “undocumented” or “illegal”. We collected ~250 participants per state x label condition as that is the sample size at which correlations stabilize (Schönbrodt & Perugini, 2013). The Texas illegal condition had 2 extra participants (N = 252) that were collected as pilot-testing participants. The average age across the full sample was 38 (SD = 12) and the gender distribution was slightly skewed towards women (53.9%). The ethnoracial distribution was as follows: white (57.2%), latinx (16%), black or African (11%), East asian (9.5%), South asian-Indian (2.7%), race or ethnicity was not listed (2.4%), Hawaiian-Pacific Islander (.9%), Indigenous-Native American (.3%), Middle Eastern (.1%). In terms of citizenship status, 92.6% were born in the U.S. and 97.8% were U.S. citizens. A geospatial map of where in each state participants resided can be seen in **Supplementary Figure S2**.

Participant measures

The following individual difference measures were used to help characterize representational variation. The full descriptive table for participant characteristics can be found in **Supplementary Table S1.** Demographic variables included *age*, *self-reported gender*, *self-reported race*, *religious affiliation*, and *education level* (Master’s or Doctoral degree, Bachelor’s degree or similar, Professional qualification, High school or Baccalaureate or A-levels, I did not complete secondary/high school).

Attitudes were measured using the *Illegal Immigrant Scale* (IIS) (Ommundsen et al., 2014). The scale included 20 statements whereby participants responded with how strongly they agreed with each one (agree strongly, agree, undecided, disagree, disagree strongly). The original scale used the "illegal" label, so we changed the wording of the statements to "unauthorized immigrants" so that the scale did not differentially match or mismatch across our label conditions. Statements ranged from economic ("*Unauthorized immigrants should not receive food stamps*"), to political ("*Unauthorized immigrants who give birth to children in the United States should be made citizens*"), to social ("*Unauthorized immigrants should not be discriminated against*"). Scores were computed by averaging the responses after reverse coding the relevant items. Scores ranged from 1 (positive) to 5 (negative) attitudes (M = 3.00, SD = .30).

There were four political ideology and affiliation variables: *political party affiliation* (Democrat, Independent, Republican, Green, Libertarian, Unaffiliated/Not political), *presidential vote in 2016* (Hillary Clinton & Tim Kaine: Democratic Party, Donald Trump & Mike Pence: Republican Party, Gary Johnson & Bill Weld: Libertarian Party, Jill Stein & Ajamu Baraka: Green party, other candidate, could not vote, chose not to vote), *support for building a wall* along the U.S.-Mexico border (agree strongly, agree, undecided, disagree, disagree strongly), and *political orientation*. Political orientation was measured using the Social and Economic Conservatism Scale (SECS) (Everett, 2013). Participants were presented with 12 political issues (e.g., "*abortion*", "*patriotism*", "*traditional marriage*") and asked to designate on a thermometer scale from 1 (negative) to 100 (positive) how they feel about it. Scores were computed by reverse coding the relevant items and averaging the responses. Higher numbers indicate more conservative orientations (M = 59.5, SD = 17.4).

Social geographic variables included: *state* lived in, *how long they lived in that state* (Less than 1 month, Less than 1 year, Over 1 year, Over 10 years), estimates of *frequent contact with immigrants*, subjective *estimates of the size of the surrounding illegalized immigrant population*. While data collection was restricted to only Texas and California, 14 participants completed the task from another state. We kept them in the analyses and labeled their state as "Other". Most of the sample lived in their state for over 1 year (8.7%) or over 10 years (90%). Since immigrant status cannot always be readily perceived in fleeting daily social interactions, immigrant contact was assessed by having participants write down the initials of up to five immigrants they are in frequent contact with. Contact scores were calculated by the number of names they wrote down. Text input was processed to exclude non-name responses (e.g., statements that they do not know any immigrants). Population size estimates were calculated at three levels: their neighborhood, their city, and their state. The question asked was "*Of all the people living in the location above, what percentage do you think are unauthorized immigrants?*". The order of the three locations was randomized and each location was estimated separately. The options were displayed as percentages from 0% to 50% in increments of 5 with the final option being "more than 50%", however values in between could be chosen as the value of the slider was displayed above the scale and updated as the slider was moved ($M_{neighborhood}$ = 12.5%, Median = 5%, SD = 14.5; M_{city} = 19%, Median = 15%, SD = 15.2; M_{state} = 24.6%, Median = 21%, SD = 15.1). To put these estimates into perspective, the national illegalized population size in 2016 was 3.3% with Las Vegas having the largest population (8.2%) and Philadelphia having the lowest (2.6%) (Pew Research Center, 2019a). Keeping in mind the difficulty of enumerating this population and the uncertainty surrounding these statistics, the size of the surrounding illegalized immigrant populations seems to be overestimated, particularly for larger geographic zones.

A correlation matrix that describes the relationships between all continuous participant measures can be seen in **Supplementary Figure S3**. Most variables were weakly correlated except the three population size estimation measures.

Procedure

After providing consent, participants completed a standard reverse correlation task. They were asked to visualize either "illegal immigrants" or "undocumented immigrants" followed by

300 forced choice trials where they decided which of two presented face stimuli looked more like the visualized target. They pressed the "0" key for the right face and the "1" key for the left face. The stimuli were presented at 9 cm x 9 cm and side-by-side on screen. Trials were self-paced and a 1 second fixation cross appeared after each trial. After the task, participants completed the individual difference questionnaires.

Stimulus generation

The base face was a morph of all the male faces in the London Face Database (DeBruine & Jones, 2017). Overall, 770 stimuli were generated by repeatedly superimposing random noise over the base face using the rcicr package (Dotsch, 2017). Out of 770 generated face stimulus pairs, only the first 300 were used for this study.

Classification image generation

Individual and average classification images were generated using the rcicr package. To generate individual classification images, the noise pattern of the chosen face stimuli was averaged. For the average classification images, the noise patterns of the individual-level classification images were averaged across the sample, across participants within different levels of variable, or across participants within a cluster depending on the analysis.

Image analyses

Analytic pipeline

Representational similarity. The first step is to compute a matrix that characterizes inter-individual representational similarity. This matrix was computed by first isolating the pixel noise pattern from each participants' classification image, estimating their idiosyncratic mental representation (**Figure 1a**). The base face is not used in this analysis, diverging from related analyses (Hong & Ratner, 2020), since it is typically added to the noise pattern to create all classification images and therefore adds no additional information and would inflate similarity between individuals. The noise pattern itself contains irrelevant pixel information that can also inflate similarity (e.g., the background around the face), so these pixels were removed by using an oval mask that isolated the area of the face. The masked noise pattern was then turned into a vector. All participants' masked noise vectors were then correlated and placed into a participant x participant similarity matrix (**Figure 1b**). This correlation matrix was then transformed into Euclidean distances for the clustering analysis.

The similarity estimation detailed above is an extension of representational similarity analyses (RSA) in neuroscience that calculate correlations between brain images' pixel intensities (Kriegeskorte et al., 2008). Within RSA analyses and reverse correlation studies (Brinkman et al., 2019; Dotsch & Todorov, 2012), similarities between images are typically calculated using Pearson correlations between pixel vectors. Other similarity functions like Euclidean or Mahalanobis distance (Bobadilla-Suarez et al., 2018; Kriegeskorte, 2019; Oh et al., 2021) or structural similarity index (Wang et al., 2004) can be used, although each make different assumptions that should be considered when comparing face images. For example, correlations quantify the similarity between trends or shapes while disregarding mean pixel intensity (e.g., may cluster representations mainly by similar facial structures than skin tones). Euclidean distance sums intensity differences between pairs of pixels and therefore accounts for mean intensity differences between images while being insensitive to dependencies between pixels (e.g., may cluster representations mainly by similar skin tones than facial structure) (Aly et al., 2008). The structural similarity index accounts for luminance, contrast, and structure differences between images (Wang et al., 2018). Choice of similarity function will depend on the investigated context, what aspects of faces are deemed important to compare, and computational feasibility. Dimensionality reduction could also be considered, such as comparing similarities of significance maps rather than pixels (e.g., van Rijsbergen et al., 2014). However, more research is needed here to identify best practices.

Cluster analysis. There are many clustering methods available, two popular ones include partitioning clustering (i.e., K-Means) and hierarchical clustering (King, 2015). These are unsupervised because they take unlabeled datasets as inputs and iteratively attempt to find and optimize cluster assignments based on structure in a distance (i.e., dissimilarity) matrix. Partitioning methods start with an initial partition and continuously reassign observations to clusters as the algorithm proceeds. They require declaring the number of clusters the algorithm should find, a benefit when the representational space is already known. Hierarchical methods produce clusters by permanently and sequentially combining or dividing pairs of observations using a similarity criterion. The number of clusters does not need to be declared upfront as it is up to the researcher to post-hoc identify the appropriate number. Given that representational schemas for illegalized immigrants is a relatively unexplored space, we decided to use hierarchical clustering for three reasons: it does not require an a priori decision about the number of clusters (various cluster numbers can be explored afterwards), the process is deterministic and thus arrives at the same solution, and the clustering process is depicted on a dendrogram which provides a temporal visualization of the clustering decisions (**Figure 1c**). Despite these advantages, there are many algorithmic options and decisions to be made when running a hierarchical clustering algorithm (Yim & Ramdeen, 2015). We explored a few options to find reasonable parameter settings for our application.

First decision is whether the hierarchical clustering algorithm should start with smaller clusters and iteratively build up to larger ones by finding the most similar clusters (i.e., agglomerative), or start with one giant cluster and break down to smaller clusters by finding the most distinct clusters (i.e., divisive). Whereas the former better identifies smaller clusters, the latter better identifies larger clusters. Since the goal was to identify clusters of similar representations that may not necessarily be large, we chose agglomerative clustering. The next important decision is which metric (i.e., “linkage”) should be used to measure similarity between observations when iteratively deciding which observations to cluster together. We tested which of three linkages led to a solution with clearly distinct clusters (**Supplementary Figure S4**). The participant similarity matrix was transformed into a Euclidean distance matrix and fed into a hierarchical algorithm with one of three linkage functions: average linkage, complete linkage, or Ward’s method. The average linkage measures the distance between the average similarity within two clusters. The complete linkage measures the distance between the furthest observations from each cluster. Ward’s method instead minimizes the total within-cluster variation. We compared two cluster metrics for each linkage method: the agglomerative coefficient (AC) and the sample sizes of the resulting clusters. The AC is a measure of how much cluster structure is found with a range from 0 (weak) to 1 (strong). A good cluster solution would show strong clustering structure. The ACs were as follows: average linkage AC = .56, complete linkage AC = .77, Ward AC = .96. A secondary metric we used was sample size (**Supplementary Figure S5**): the goal was to find an algorithm where the minimum sample size in any of the clusters would not be too low to obtain a reliable average image. Ward’s method was the only algorithm that stayed consistently above 20 minimum participants as recommended (Dalmaijer et al., 2020) and provided a strong cluster structure. While we focus on Ward’s method, we also computed the same pipeline (e.g., clusters and average representations) for the complete linkage method with the goal of comparing the two. Therefore, the faces from the complete linkage pipeline are part of the rating task below. However, since clusters were not as differentiated using complete linkage, those results are not analyzed further.

The last critical choice is to decide how many clusters exist or are meaningful to examine. To aid in comparing cluster number solutions, we used two metrics: total within-cluster sum of squares (TWSS) and minimum cluster sample size. Clusters with smaller TWSS have more similar observations, which is ideal and exactly what Ward's method optimizes. However, a cluster with two or three people can also optimally minimize TWSS, therefore it is important to consider the TWSS in combination with minimum sample size. The goal is to find clusters with low TWSS and a minimum sample size of "N=20 to N=30 per expected subgroup" when clusters are distinguishable (Dalmaijer et al., 2020). Considering the TWSS and minimum sample sizes together suggested that between 5 to 15 clusters would be reasonable solutions to explore (**Supplementary Figure S5** and **S6**). Less clusters would yield higher TWSS, any more clusters and the results would be harder to summarize and sample sizes would be too low. More research is needed on optimizing multiple sample size considerations in data-driven approaches that sequentially combine cluster analyses with machine learning classification models.

Since there is no known a priori solution to compare to, we instead ran the same analytic pipeline to compare 5, 10, and 15 cluster solutions as a comparative analysis to see what insights could be gleaned from more or less cluster partitions. We focus on reporting the 5 cluster solution as it showcases the main conclusions we can take away from the data-driven approach without the complexity of discussing more clusters. This choice does not mean the 5 cluster solution is the best, just the simplest to report. However, results from the 10 cluster (**Supplementary Figure S7, S8, S9**) and 15 cluster (**Supplementary Figure S10, S11, S12**) are reported in the supplementary materials. We also summarize any differences found from changing cluster numbers in the results section.

Validation

Cluster validation occurred by characterizing the content of each cluster's average representation and examining which variables tracked cluster membership. A common validation metric for machine learning models is predictive accuracy on held out samples, however, for these data, hold out accuracy was low. For researchers interested in generalizable findings, improving predictive accuracy is important, otherwise the computed clusters and variables differentiating those clusters may not replicate in other samples. One reason for the low accuracy could be the reliability of the classification images. If classification images do not contain meaningful signal (e.g., random responding), cluster results may be driven by noise. In the absence of repeated classification trials to compute test-retest reliability, one could compute an infoVal which quantifies the informational value of a classification image compared to a null distribution (Brinkman et al., 2019). Factors that influence infoVal scores are number of classification trials and proportion of random responses. Less random responses and more trials will yield higher infoVal scores (i.e., more signal), but not always: increasing trials can induce more random responding due to demotivation. The significance cut-offs mirror those of z scores (1.96 and 3). Our sample's infoVal scores ranged from -2.4 to 8 (Supplementary Table S1), however we report this metric cautiously in this context since the infoVal is more sensitive to local than diffuse signal in an image and has been mainly validated using gender categories and light-skinned base images where skin tone (a diffuse signal) was not a primary signal. Model selection can also affect predictive accuracies: more powerful and complex models (XGBoost or deep learning) could potentially improve predictive accuracies, but at a cost to interpreting the model. Another reason may be cluster imbalances: when clusters differ greatly in size, classification algorithms learn to optimize accuracy by guessing only the largest cluster. This means predictive accuracy in the case of imbalanced clusters reflects information about the distribution of cluster sizes instead of validity (Akosa, 2017). Weighted sampling (described below in the random forest methodology) can help minimize these imbalances.

However, high predictive accuracy may also not be an appropriate goal for our application. There are many domains where using machine learning techniques for qualitative descriptions is valued over generalizable prediction (Bratko, 1997). This is especially helpful when the investigative context is not well known and it is beneficial to explore, as qualitative understandings gained from machine learning computations can spur new hypotheses to investigate. We consider the development of this new analytic pipeline to characterize understudied representations of illegalized immigrants a good example of an unknown space in need of exploration through qualitative computations. We therefore do not assume that identified clusters will generalize beyond our sample, but plan to follow up on interesting patterns in future investigations. Moreover, given that it is unknown how many clustered schemas of illegalized immigrants exist in society, it was important to treat cluster assignments as probabilistic (i.e., the probability of a participant belonging to each cluster) rather than through the lens of classification accuracy (i.e., a forced decision that each participant singularly belongs to one known cluster) (Harrell, 2017). In these ways, the low predictive accuracies may not be a problem for this study.

Cluster content. For each identified cluster, an average classification image was computed (**Figure 1d**) and rated on various traits (**Figure 1f**), see image rating task details below.

Cluster membership. Cluster membership was characterized using two supervised learning classification models (i.e., cluster labels are provided): decision trees and random forests. The decision trees used in this study were conditional inference trees with the partykit package version 1.2.11 (Hothorn et al., 2006). The algorithm conducts an exhaustive search through all variables and their constitutive levels to find the partitions that maximally differentiate cluster membership. At each step, it first conducts a general null hypothesis test that any of the variables predict cluster membership – the one with the lowest p value gets placed as the initial partition variable. Then the algorithm searches through all the levels of the chosen variable and conducts more null hypothesis tests searching for the lowest p value to create a split, suggesting the resulting probabilistic cluster memberships are more differentiated across the partition. The search continues through variables and variable levels until there are no more significant splits. The resulting decision tree provides a summary map of the search. The recursive nature of the search allows for an easy exploration and identification of complex interactions between variables. The model options were as follows: tests were corrected using Bonferroni correction, the alpha level was .10 to facilitate exploration, the split statistic was "quadratic".

The descriptive advantage of decision trees' exhaustive search is associated with a high possibility of overfitting. Random forests can mitigate this issue by combining multiple decision trees to provide a more robust idea of which variables are important and how (Breiman, 2001a). The algorithm uses similar procedures for creating decision trees, however randomness and bootstrapping are embedded into the process. First, a random subset of the variables is chosen to search through, this creates more varied trees because the most important variables are not always the initial split. Second, a random subset of the data is held out of the search to also ensure tree variation and assess out-of-bag predictive accuracy. Third, for imbalanced clusters, there are procedures for weighting observations or under- and over- sampling them to try to create better cluster balance (Chen et al., 2004). Lastly, techniques for exploring variable interaction effects in random forests are less developed (Molnar, 2020), so we focus on confirming the importance of single variables.

Random forests were computed with the ranger package version 0.12.1 (Wright & Ziegler, 2017). To minimize cluster imbalance, observations were probability weighted (e.g., observations in larger clusters were proportionally less likely to be chosen for the subset training samples). Since random forests combine across trees, reporting single trees would not be representative of what the model ultimately learned. Instead, we report variable importance metrics, specifically a permutation p value that compares observed predictive accuracy to predictive accuracies from null distributions made by repeatedly shuffling cluster labels (Altmann et al., 2010). Variable importance only provides an idea of which variables are useful predictors; we also need to know how they map unto cluster membership. For understanding the variable-cluster mappings that the models learned, we report partial dependence plots (PDP) (Apley & Zhu, 2020; Molnar, 2020). These values are analogous to estimated marginal means in regression models - they plot how the average predicted probability of membership in each cluster varies across levels of a variable. However, there exists no statistical inference techniques for these estimates, so they remain descriptive in this study.

As initial proof that our measures are valid and that random forest models can capture meaningful relationships, we tested which variables were related to support for building the Mexico-U.S. wall. The 2016 presidential vote, political orientation, and political party affiliation were identified as important variables for predicting support for building the wall in the expected directions (**Supplementary Figures S13 and S14**). These results build confidence that patterns found in the main analyses are meaningful.

Image rating task

Participants

There were four sets of raters for this portion of the study collected in May 2020. Previous simulation power analyses suggest 20 participants provided enough power for ratings (Martinez, Oh, et al., 2021a, 2021b). However, data from those studies also showed that test-retest reliability of ratings tends to be lower for classification images. To compensate for unreliability exclusions (i.e., a negative test-retest correlation), we collected more participants. The differences between the total number and the final number in the following sample sizes are due to reliability exclusions. Participants rated classification images on dangerousness (N_{total} = 60, N_{final} = 46, M_{age} = 38.3, SD = 10.4, 14 women, 32 men), Americanness (N_{total} = 60, N_{final} = 46, M_{age} = 40.2, SD = 12.9, 22 women, 24 men), dominance (N_{total} = 59, N_{final} = 44, M_{age} = 36.9, SD = 12, 19 women, 25 men), or categorized them on their perceived ethnoracial membership (N_{total} = 97, N_{final} = 87, M_{age} = 38.1, SD = 12.4, 33 women, 54 men). Overall, 96% of the raters were born in the U.S. and on average scored near the midpoint of the social and economic conservatism scale (M = 58.9, SD = 20.3). Full sample characteristics can be found in **Supplementary Table S2**.

Procedure

Participants were sequentially presented with 61 average classification images derived from the various cluster algorithms (complete linkage vs. Ward's method) and number of clusters described above (5, 10, 15) and asked "*How [dangerous, American, dominant] is this person?*". Participants only evaluated one trait from 1 (not at all) to 9 (extremely). For ethnoracial categorization, participants saw each face separately and were asked "*What race/ethnicity is this person?*" with five options: asian, black, latino or Hispanic, Middle Eastern, or white. The set of face stimuli for all the ratings were randomized. Each face image was presented at 300 pixels x 300 pixels. All trials were self-paced and there was a 250 ms delay before the next trial. All images were repeated and rated a second time to assess test-retest reliability. Reliability was greatest for ethnoracial categorization (Mean r= .47, SD = .23, followed by dangerous (Mean r= .35, SD = .21, American (Mean r= .37, SD = .20, and dominant (Mean r= .30, SD = .24) ratings.

Analyses

Trait ratings were analyzed using mixed effect regression models in the lme4 package (Bates et al., 2015). Ratings were predicted by a face-cluster variable, random intercepts by participants and by the interaction between participants and faces to account for the repeated measures by participants and ratings given to each average face. Satterthwaite approximations were used to calculate degrees of freedom (Luke, 2016). Marginal means, two-sided pairwise comparisons of the average trait ratings given to each face, and effect sizes (Cohen's *d*) were estimated using the emmeans package version 1.5.3 (Lenth, 2020). Comparisons were corrected for false discovery rate. Since we focused on the 5 cluster solution using Ward's method, we extracted and report those specific estimates from the full model. The ethnoracial classification ratings were descriptively summarized with a percentage of the sample that responded each category per face. The top two categories and their percentages are shown for each of the cluster faces in the figures.

Results

Theory-based approach

To illustrate issues with the theory-based approach, **Figure 2** displays the average classification image for the full sample, the four main state-label conditions, and various levels of political orientation. The five score ranges on the SECS were chosen to reflect equidistant scores that could be interpreted as meaningfully different levels of political orientation (i.e., numbers closer to the ends are more politically extreme than numbers closer to 50). A visual examination could lead researchers to infer that a dark-skinned person is a shared representation held by most participants no matter the labels, state, or political orientation– a similar face was produced across all the variables. The one exception is the image produced by very liberal participants in the upper-right corner which might suggest liberals hold a different understanding of illegalized immigrants. This exception also averages across only 30 participants and is not visible within the faces from the state-label conditions even though they are all derived from the same set of participants. This suggests smaller sample sizes can produce representations that are occluded when averaged into a larger sample. Researchers would need to investigate all potentially relevant variables to find hidden representational variation, a very costly endeavor given the multi-component structure of the typical reverse correlation task (image generation and image ratings). Such an endeavor may even prove futile if single variables fail to capture representational similarities by assuming cohesiveness. For instance, some extreme liberals may produce a similar face as some extreme conservatives which would go unnoticed if they are instead averaged with others who share a political orientation. This example situation *would* be accounted for by the data-driven approach which instead relies on probabilities to describe the relationships between variables and representations.

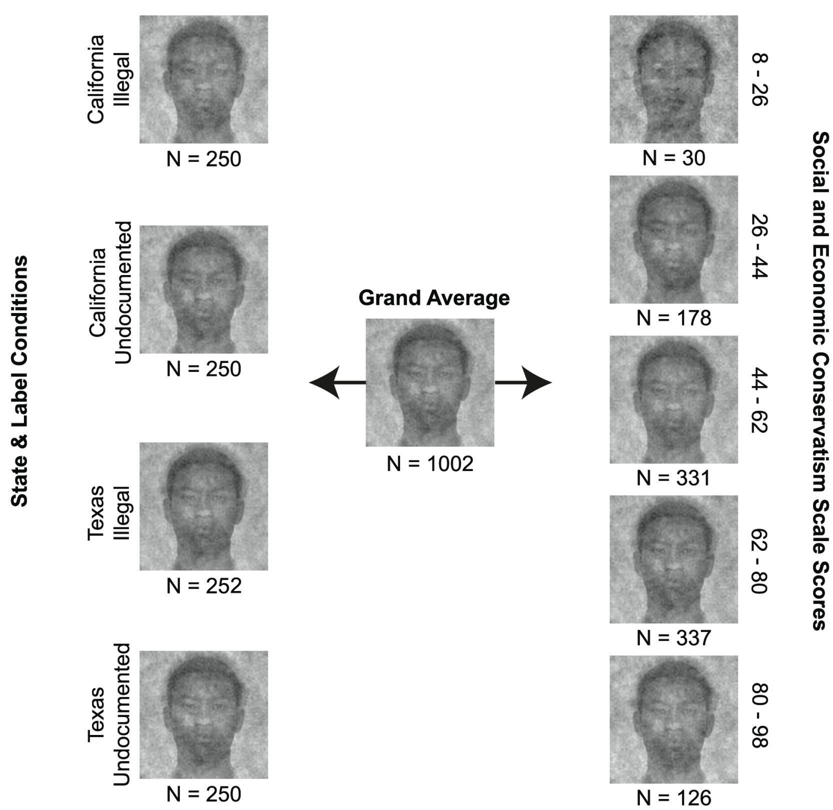

Figure 2. Average classification images using a theory-driven approach. The center face reflects the average classification images across the full sample (i.e., grand average). The left side shows how the grand average image partitions into average faces for the various state-label conditions, the right side partitions the grand average into various levels of the social and economic conservatism scale (higher numbers reflects more conservative participants). The number at the bottom represents the sample size of each average face.

Data-driven approach

Cluster content

The five-cluster solution led to imbalanced clusters. In terms of percentage of the sample, Cluster 1 was the largest (38%), followed by Cluster 2 (22%), Cluster 3 (17%), Cluster 4 (16%), and Cluster 5 was the smallest (7%) (**Figure 3a**). The average cluster classification images were phenotypically different across clusters (**Figure 3b**), however it's important to understand how they differ in terms of elicited social evaluations (**Figure 3c**).

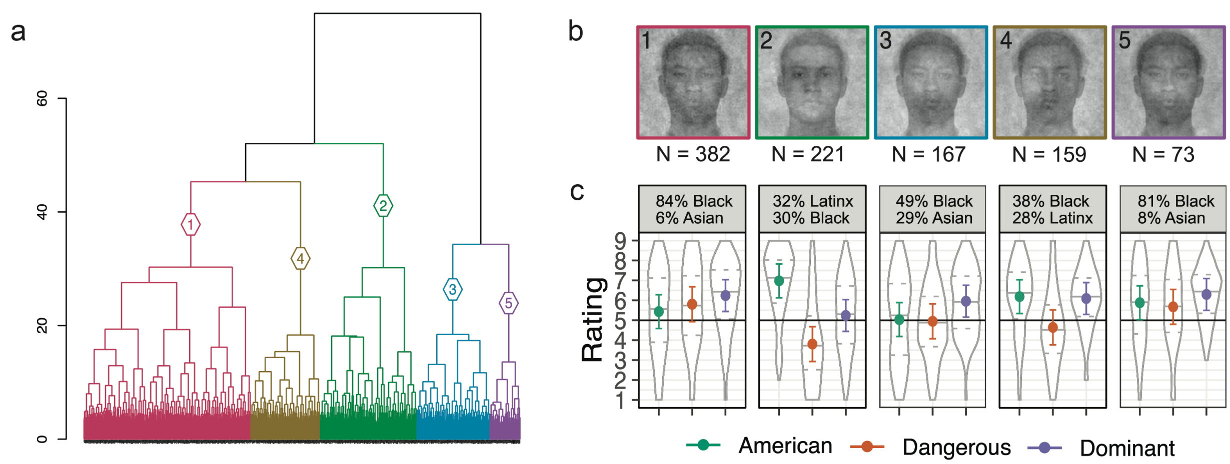

Figure 3. Five cluster solution from the hierarchical clustering analysis. a. Dendrogram depicting the five clusters in various colors. **b.** The average faces and sample sizes from each cluster (number and color coded to match the dendrogram). **c.** Race and trait ratings of each cluster's average face. The percentages in the grey box reflect the top two ethnoracial classifications. The plots show estimated marginal means from the trait ratings. The error bars depict 95% confidence intervals. The violins display the distributions of rating data while the dashed lines represent quartiles. The horizontal line is the neutral scale position (5) of each rating.

The following results will not report traits whose estimated means and confidence intervals crossed the neutral rating (5), suggesting that trait was on average less critical for characterizing that cluster's representation. Cluster 1 contained a representation perceived as somewhat dangerous (M= 5.80 CI[5.30, 6.31]), dominant (M= 6.24 CI[5.44, 7.04]), and mostly categorized as black. Cluster 2 instead contained a representation perceived as very American (M= 6.98 CI[6.13, 7.83]), not dangerous (M= 3.80 CI[3.30, 4.31]), and a mix of Latinx and black. Cluster 3 was perceived as mostly dominant (M= 5.96 CI[5.16, 6.75]) and a mix of black and Asian. Cluster 4 was perceived as American (M= 6.19 CI[5.34, 7.04]), dominant (M= 6.09 CI[5.29, 6.89]), and a mix of black and Latinx. Cluster 5's representation was perceived as American (M= 5.88 CI[5.03, 6.73]), dominant (M= 6.29 CI[5.49, 7.09]), and mostly black.

Pairwise cluster comparisons of the ratings corroborated the cluster-specific content. Cluster 2 was perceived as the least dangerous representation (bs_{range}= [.84, 2.0], ds_{range}= [.41, .97], ps_{range}= [<.0001, .003]), Clusters 1 and 5 as the most dangerous (bs_{range}= [.73, 2.0], ds_{range}= [.35, .97], ps_{range}= [<.0001, .009]). Clusters 1, 3, 4, and 5 were perceived as similarly dominant (bs_{range}= [.05, .34], ds_{range}= [.03, .19], ps_{range}= [.290, .808]) and all more dominant than Cluster 2 (bs_{range}= [.72, 1.06], ds_{range}= [.40, .59], ps_{range}= [.0001, .006]). Cluster 2 was perceived as the most American representation (bs_{range}= [.79, 1.95], ds_{range}= [.41, 1.00], ps_{range}= [<.0001, .005]). Cluster 4 was perceived as more American than Cluster 1 (*b*= .75 CI[-.01, 1.51], *d*=.38, *p*=.008) and Cluster 3 (*b*= 1.15 CI[.40, 196], *d*=.59, *p*=.0001). Cluster 5 was perceived as more American than Cluster 3 (*b*= .85 CI[.09, 1.6], *d*=.43, *p*=.003). All other comparisons were not significant (*ps*>.122).

To summarize and interpret, Clusters 1 and 5 are dark-skinned threat representations. Clusters 2 and 4 operate as non-threatening representations, although Cluster 2 is lighter skinned and less threatening than Cluster 4. Cluster 3 is a dark-skinned dominant representation, the most evaluatively neutral out of all the clusters. Cluster 4 and Cluster 3, to a lesser extent, paint a nuanced picture of collective schemas of illegality and racialization because they suggest that darker skin is not always represented or perceived as negative (e.g., Alter et al., 2016). These results provide evidence of representational variation in understandings of illegalized immigrants – some are positive, some are negative, and they vary in skin tone and facial features, suggesting people might be trying to visualize specific nationalities or race categories (Martinez, Oh, et al., 2021b).

Cluster membership

Representational content alone is insufficient for validating clusters since even subtle differences between face images can lead to different evaluations. Validation here then further relies on identifying which variables track cluster membership and if those variables theoretically match the representational content of that cluster.

<u>Decision tree.</u> The decision tree provides a descriptive picture of which variables are important predictors of cluster membership and how they interact. The tree shows that age is the most important predictor, followed by estimates of the size of the illegalized population in one's neighborhood, followed by the state where participants live (**Figure 4**). The cluster distribution in the bottom figures suggests that the collection of variables do not maximally differentiate between clusters, so our analytic inferences focus on relative probabilities. Moreover, it should be noted that Cluster 1 will always show the largest probability as it was the largest cluster, so inferences will specifically focus on relative probabilities of the other clusters.

Starting from the age variable, the first important split is between individuals who are older vs. younger than 48 years old. Older participants show a higher probability of being in Clusters 3, 2, and 5 which are a mix of neutral, non-threatening, and threatening representations. For participants under 48, the next important split is between younger participants who perceive the illegalized population size in their neighborhood to be a more or less than 26%. Those who perceive a lot of illegalized immigrants in their neighborhood are very likely to be part of Cluster

2 and 4, the non-threatening representations. Lastly, for young participants who perceive few illegalized immigrants in their neighborhoods, the next tentative split is whether they live in Texas vs. California and the other states. The subtle difference here seems to be that Californians are more likely to be in Cluster 2, a non-threatening representation, while Texans are more likely to be in Cluster 5, a threatening representation.

The decision tree provided initial evidence that the clusters *are* meaningful. Threatening representations tended to occur for older participants or younger participants in Texas who do not perceive there to be many illegalized immigrants in their neighborhoods. Non-threatening representations tended to occur for younger participants who perceive there to be many illegalized immigrants in their neighborhoods, or who perceive fewer but live in California and other states. These results highlight the importance of geographic and specific demographic variables as sources of representational variation. However, since decision trees have overfitting issues, we test the robustness of these variables in random forests.

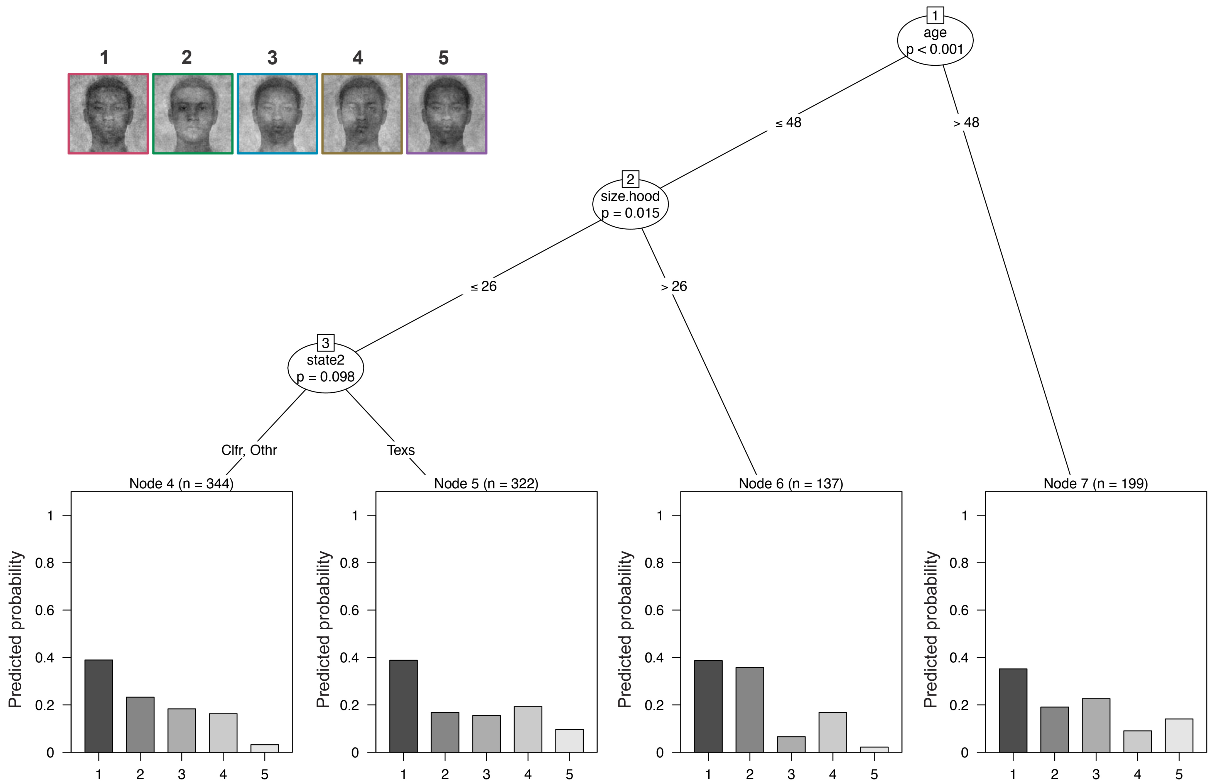

Figure 4. Conditional inference decision tree for five cluster membership. The ovals represent the most important predictor variables and their p values. The lines between variables and the bottom plots depict the level of the variables at which splits occur. The bottom plots depict the resulting probabilistic cluster membership distribution based on various tree partitions. The x-axes are the different clusters and the y-axis is the probability of belonging to each cluster. Sample sizes are provided above the plot for each partition. The top left faces are a legend to remind what each cluster represents. The “size.hood” variable is estimates of the undocumented immigrant population size in their neighborhood, “age” is the age of the participants, “state2” is the state they live in.

Random forest. The permutation p values for the importance of each variable can be seen in **Figure 5**. Only one of the variables identified by the decision tree remained significant: estimations of perceived illegalized immigrant size in one’s neighborhood (p= .030). Age (p=.079), the 2016 vote (p=.089), estimations of perceived illegalized immigrants in one’s city (p=.139), and lived-in state (p=.188) were the next highest important variables, though not significant. Since neighborhood estimates and age were consistently identified as relatively more important across analyses, we explored how they are related to cluster membership more closely.

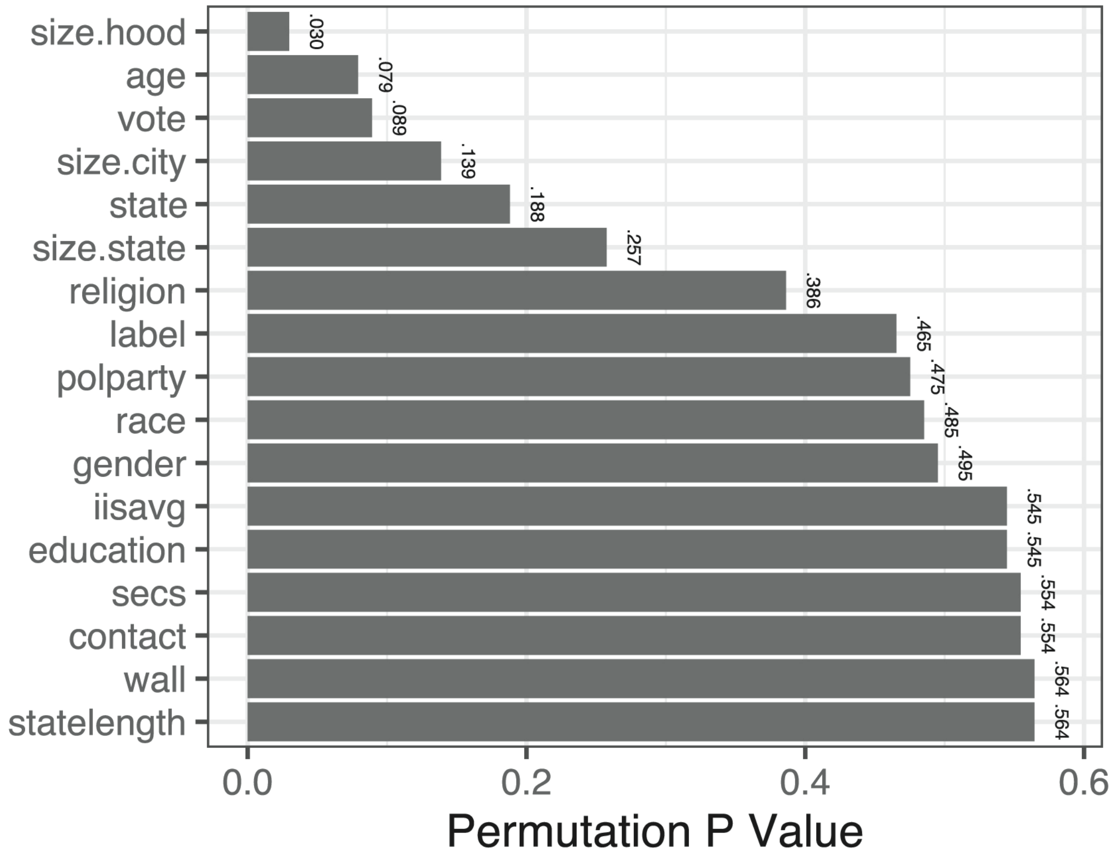

Figure 5. Permutation variable importance for five cluster solution. The x-axis is the permuted p value representing variable importance (significant alpha is .05). The exact p value is provided to the right of each bar. The y-axis lists all the individual difference measures.

Partial dependence plots suggested that the importance of neighborhood estimates occurred mainly for Cluster 2 and Cluster 3 (**Figure 6**). The more immigrants participants perceived in their neighborhood, the more likely they were to be a member of Cluster 2 (a non-threatening representation) and less a member of Clusters 1, 3, and 5 (more neutral and threatening representations). Similarly, the older the participants, the less likely they were to be part of Cluster 2 and 4 (non-threatening representations) and more likely to be a member of Cluster 3 and 5 (more neutral and threatening representations).

These classification models identified two variables as important for differentiating clusters, would we have arrived at similar conclusions if we created averages within those variables from the start? Figure 6 shows the average face produced by binning age or perceived population estimates using equidistant values within each variable (results did not change if we binned using data quintiles instead of variable equidistance). This juxtaposition highlights a few insights. First, the cluster approach allows probabilistic cluster assignments and inferences while the average approach treats one's age or population estimates as a predetermined cluster. For example, we arrive at different conclusions if we want to understand the mental representations of participants who perceive an incredible number of undocumented immigrants in their neighborhoods (over 50%!). In Figure 6A, it is very likely they will hold a light-skinned non-threatening representation (Cluster 2) and very unlikely to hold Cluster 5's representation, but this does not preclude them from belonging to any of the cluster representations. The averages from Figure 6C, however, would lead to the conclusion that these participants hold a darker-skinned (potentially threatening) face representation. This inferential difference occurs because participants with high population size estimates exist within every cluster, averaging across these participants' representations will heavily weigh the most numerically shared face representation (Cluster 1). The largest representational cluster will therefore dominate faces produced from large subsamples of participants, see Figure 6D and Figure 2. This could lead to the illusion that this representation is shared across everybody, even when there's meaningful variation.

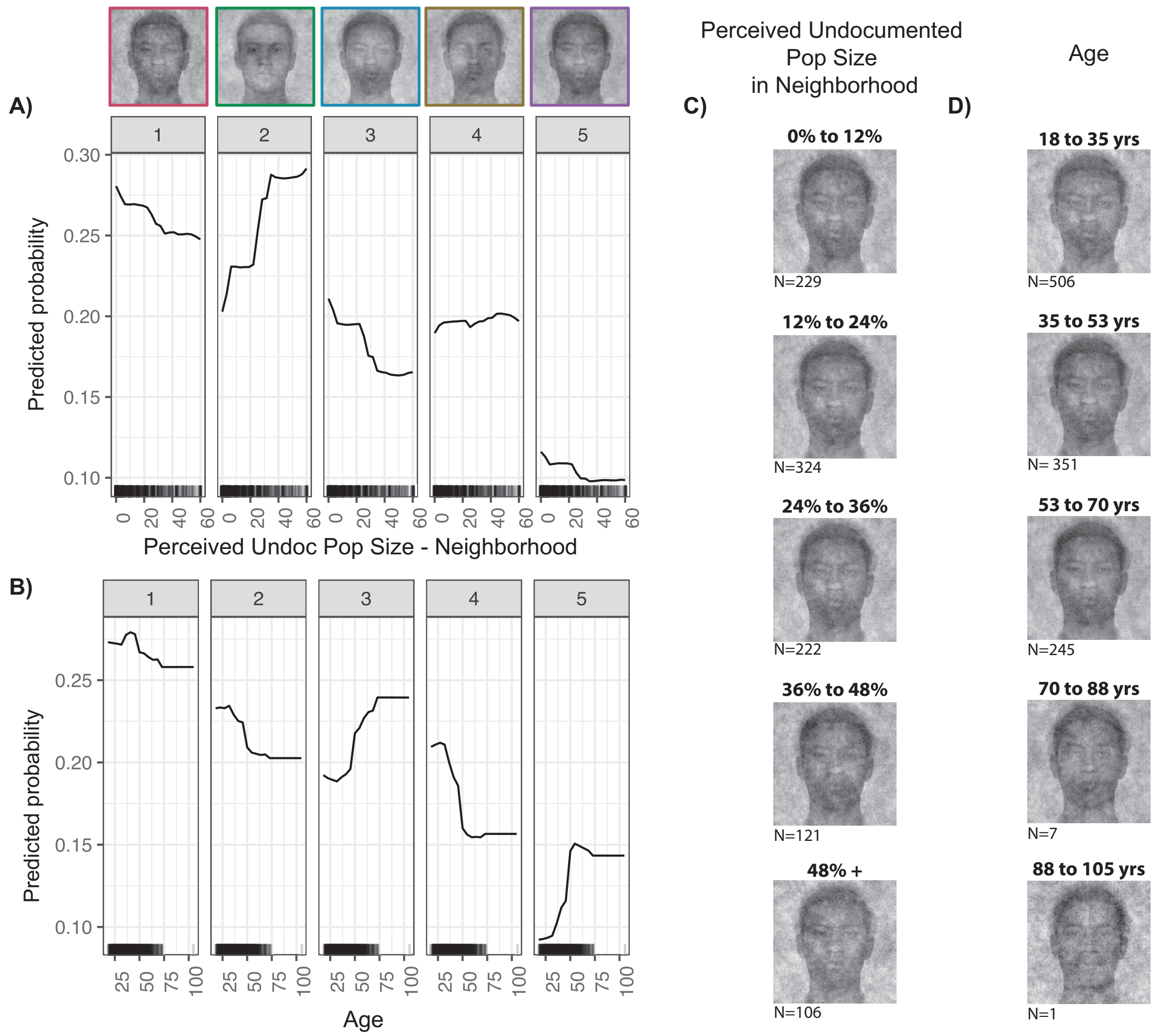

Figure 6. Partial dependence plots for five cluster solution alongside variable-derived averages. a. Probabilistic cluster membership across perceived undocumented population size in the neighborhood. **b.** Probabilistic cluster membership across age. The y-axis is the probability of cluster membership. The black tick marks above the x-axis are data points such that the less tick marks the less participants at that level of the x-axis variable. c. Average faces per equidistant bins of the undocumented population size estimate variable. d. Average faces per equidistant bins of the age variable. The number at the bottom represents the sample size of each average face.

Does the number of clusters matter?

When these five clusters are further partitioned into ten or fifteen smaller clusters, some results remained consistent while new ones emerged (**Supplementary Figures S7 to S12**). An example of a pattern that remained consistent was the partitioning of Cluster 2 in the 10 and 15 cluster solutions. No matter how many subclusters Cluster 2 was partitioned into, the resulting representations tended to be lighter skinned and perceived as highly American and non-dangerous. Smaller clusters like Cluster 3 and Cluster 4 only partitioned into two separate representations in the 15 cluster solution and those representations were given similar ratings as the larger cluster image. Cluster 5 remained intact in all the solutions. The largest cluster however, Cluster 1, was partitioned into many subclusters which revealed hidden images – some similar to the original cluster, others smiling and non-threatening, but all dark skinned. Moreover, while most of the ethnoracial classification ratings from the 5 cluster solution tended to fall along Latinx, black, and Asian categories, more subclusters resulted in some images also being perceived as white and Middle Eastern. Lastly, neighborhood size estimates and age remained important variables that predicted cluster membership for the 10 cluster solution and age for the 15 cluster solution in a way that mirrored the 5 cluster solution.

These results suggest that the correlation similarity function picks up on different features for grouping different levels of the hierarchical clustering. It appears that larger clusters are mainly grouped by global face information (e.g., skin tone) while the smaller clusters use more specific information (e.g., affective expressions). This could occur because when a cluster of images share the same global features and thus overlap highly in visual information, what differentiates pairs of faces within this cluster are more fine-grained features, like facial expressions. That results can change based on cluster number suggests some representations are internally cohesive, while other representations contain internal heterogeneity that can be further excavated. These patterns suggest lower number of clusters (i.e., larger clusters) can provide a coarse summary of representational variation within the data, yet there may be more nuanced representations at higher cluster numbers. These insights speak to the benefits of hierarchical clustering which allows post-hoc comparisons of cluster number solutions from the same dendrogram.

Discussion

With the goal of mapping varied understandings of social categories, here illegalized immigrants, this project addressed two issues with standard reverse correlation practices that can restrict inferences about mental representations. First, averages can hide meaningful heterogeneity and, second, theory-derived variables may not fully capture the social contours of collective representations. We proposed a data-driven approach that calculated inter-individual similarity in representations, identified clusters of similar representations, and characterized the extent to which variables tracked cluster membership. This approach found highly shared representations and less shared representations that were somewhat differentiated by demographic (age) and social geographic variables (population size perceptions of illegalized immigrants in one's neighborhood). We summarize the insights gleaned from this procedure followed by acknowledging limitations worth addressing in future research.

Varied schemas for illegalized immigrants

A limitation of data-driven approaches is that the resulting solutions may not always be easily categorizable or interpretable, the researcher must then reintroduce theoretical knowledge to aid in interpretation (Adolphs et al., 2016). With this in mind, we identified clusters whose average representations tended to fall along lines of threat vs. non-threat across varied skin tones. Shared features among most of the representations was darker skin and facial features perceived as dominant, suggesting these features are highly associated with illegality across more minds. Cluster 1's representation was the most shared and crosscutting and therefore was not explained by any individual difference variables. This may be why the image from Cluster 1, a dark-skinned threat, appears similar to theory-derived average classification images (**Figure 2**) and to sample-averaged representations from previous research (Martinez, Oh, et al., 2021a).

However, meaningful clusters of individuals have a different person in mind. Representations from Cluster 5 and Cluster 3 portrayed a similar appearance to Cluster 1, except Cluster 5 was more threatening than Cluster 3. Thus, Cluster 1 and Cluster 5 could be interpreted as threat representations, while Cluster 3 could be interpreted as an evaluatively neutral representation that simply highlights beliefs that illegalized immigrants are darker skinned. Representations from Cluster 2 and Cluster 4 both tended to be non-threatening, yet the former was lighter skinned and the latter darker skinned. Due to our qualitative use of the analytic pipeline, it is important to note that these clusters should be seen as examples of existing representations within our sample, not a comprehensive typology of all possible representations. Collecting a broader sample across the U.S., in other countries, and across time could provide a wider typology of existing representations and reveal further sources that contribute to variation.

Sources of representational variation

While we tested many variables theorized to be relevant to immigrant representations, none fully differentiated between clusters, and many were not significant predictors of clustered variation. Attitudes measured from normative questions about economic, political, and social aid to illegalized immigrants did not differentiate between representational clusters. Neither did political ideologies, party affiliations, or voting decisions, nor demographics like education level or religious affiliation. Race did not either, although this was potentially expected given that a categorical race measure should not be considered an explanatory variable but an illusory multidimensional product of racist practices (Fields & Fields, 2012; Helms et al., 2005; Martinez & Paluck, 2020; Sen & Wasow, 2016). Lastly, the label used to name illegalized immigrants also did not matter here, in line with the assertion that “undocumented” and “illegal” are too criminalized that they both conjure similar representations (Martinez, Oh, et al., 2021a; Plascencia, 2009).

Our models instead revealed that Cluster 1's crosscutting racialized representation could not be explained by any of the measures, suggestive of a common influence like media (e.g., Martinez, Feldman, et al., 2021), while the rest of the clusters were differentiated by more idiosyncratic sources: age and geographic characteristics. Specifically, older participants tended to be more associated with clusters that contained either neutral or threatening and darker-skinned representations of illegalized immigrants. Younger participants instead tended to be associated with more non-threatening representations that varied in skin tone. Similarly, participants who perceived there to be many illegalized immigrants in their neighborhood were more associated with non-threatening representations, those who perceived less were more likely to hold threatening representations. The same patterns did not occur for perceptions at the level of the city or the state, suggesting that representations are highly influenced by very localized spaces.

Although we did not assess interactions between these variables in the random forests, the decision tree did suggest that age and neighborhood estimates interacted such that the cluster membership of younger participants with high neighborhood immigrant estimates tended to hold the most non-threatening representations (i.e., Cluster 2 and 4). Likewise, there seemed to be a tentative interaction with state such that those younger participants with smaller neighborhood immigrant estimates in Texas held more threatening representations than those in California, in line with each state's general political environment against or for immigrants. These results converge with policy surveys of white respondents suggesting that those who lived around more latinxs tended to favor less restrictions for illegalized immigrants, whereas those who were embedded in older-aged social networks favored more restrictions against illegalized immigrants (Berg, 2009).

These results suggest that reverse correlation is not simply a measure of attitudes but can reflect participants' context-informed expectations about people's appearances. People's local "face diet" develops or constrains visual mental representations (Dotsch et al., 2016). Fittingly, it is specifically estimates from local environments (e.g., neighborhood) that are salient in perceptions of demographic population sizes (Wong, 2007). Unfortunately, we did not collect measures of how long participants resided in the same *neighborhood*. However, most of the participants lived in their *state* for over 10 years indicating how age plays a role in population size estimates. Age as a variable confounds many age-related influences (North, 2019), yet within our analyses it may function more as a proxy measure for the amount of experience with local geography as opposed to clear-cut life stages or generational cohort effects. Those who lived in their state longer were on average older, their longer presence in a specific geo-political region had greater chance to shape their perceptions of their local social environment.

It is theorized that the diversity of local environments tunes mental representations such that more diversity leads to less differentiated evaluative representations of social groups (Bai et al., 2020). Correspondingly, participants who estimated more illegalized immigrants in their neighborhoods tended to represent illegalized immigrants as phenotypically diverse yet similarly non-threatening. The majority of these participants also lived in their state for over 10 years, suggesting they potentially adjusted to local diversity (Ramos et al., 2019). Conversely, participants who perceived less immigrants in their neighborhoods instead held more varied representations both phenotypically and evaluatively, indicative of more differentiated stereotypes. Yet, if estimates of local illegalized immigrants are low, how might their representations have developed? Although visibility can be dangerous for illegalized immigrants (Asad, 2020) and interaction with illegalized immigrants can be perceived as rare (Martinez, Oh, et al., 2021a), people may draw from available social representations (e.g., media portrayals) to profile specific people in their local environments as illegalized immigrants and update their mental representations accordingly (Romero, 2006).

Limitations

While theory-based approaches have critical limitations, so do data-driven approaches. One disadvantage is that there is no baseline answer about how many representational schemas of illegalized immigrants exist. Inferences must instead be made from exploring a range of cluster numbers, similarity metrics, clustering algorithms – from which we examined a restricted range due to the high cost of exploring the complete parameter space. Therefore, while this approach was used to extend our knowledge of variation in representations of illegalized immigrants, the procedure itself could be better validated using social categories with clear and known visual prototypes (e.g., age groups).

Another limitation is how less important variables may be influential through indirect means. For example, while political orientation contributed little to representational variation, agenda-laden media consumption could hypothetically influence estimates of immigrant population sizes and subsequent visual experiences.

Lastly, big data-driven approaches cannot easily provide a mechanistic understanding of why variables relate the way they do or of the content of clusters without the combined aid of immersive insights gleaned from theory and additional sources of data (Grigoropoulou & Small, 2022). For example, while this study focused on classifying clusters of representations, the goal is not to essentialize people with certain traits or experiences as necessarily possessing specific representations or beliefs. It is critical to further examine the processes by which some younger or older individuals and those who perceive various amounts of immigrants in their neighborhoods come to develop different and racialized understandings of illegalized immigrants that shape their visual expectations (Martinez, in press). The current classification analyses therefore only provide an initial clue: a map of shared and idiosyncratic understandings, even if only temporary or contingent. A contextual and processual account of the development of these representational clusters is additionally required for understanding why these relationships exist at all.

Conclusions

We have shown that inverted data-driven approaches are a viable way to map the diversity in representations of illegalized immigrants and how they pattern across people. Machine learning analyses revealed sources of representational variation that can go unnoticed by standard practices: representations of illegalized immigrants are not necessarily all dark-skinned threats, there exists variation in encoded facial valence and appearance that is clustered by demographic and social geographic differences. This was an initial attempt at mapping variance and can likely be improved, but the results highlight a critical need to place representational variation at the forefront of investigations of mental representations. Variation is foundational, ubiquitous, and its mapping can uncover important insights (Kahneman et al., 2021; Martinez et al., 2020). Overlooking meaningful heterogeneity can lead researchers to publish caricatures of the public and their beliefs (Martinez & Paluck, 2020).

References

Abrajano, M., & Hajnal, Z. (2015). *White backlash: Immigration, race, and American politics*. Princeton University Press.

Ackerman, E. F. (2013). The Rise of the "Illegal Alien." *Contexts*, *12*(3), 72–74. https://doi.org/10.1177/1536504213499883

Adolphs, R., Nummenmaa, L., Todorov, A., & Haxby, J. V. (2016). Data-driven approaches in the investigation of social perception. *Philosophical Transactions of the Royal Society B: Biological Sciences*, *371*(1693), 20150367–20150367. https://doi.org/10.1098/rstb.2015.0367

Akosa, J. (2017). *Predictive Accuracy: A Misleading Performance Measure for Highly Imbalanced Data*. 12.

Alter, A. L., Stern, C., Granot, Y., & Balcetis, E. (2016). The "Bad Is Black" Effect: Why People Believe Evildoers Have Darker Skin Than Do-Gooders. *Personality and Social Psychology Bulletin*, *42*(12), 1653–1665. https://doi.org/10.1177/0146167216669123

Altmann, A., Toloşi, L., Sander, O., & Lengauer, T. (2010). Permutation importance: A corrected feature importance measure. *Bioinformatics*, *26*(10), 1340–1347. https://doi.org/10.1093/bioinformatics/btq134

Aly, S., Tsuruta, N., & Taniguchi, R.-I. (2008). Face recognition under varying illumination using Mahalanobis self-organizing map. *Artificial Life and Robotics*, *13*(1), 298–301. https://doi.org/10.1007/s10015-008-0555-z

Apley, D. W., & Zhu, J. (2020). Visualizing the effects of predictor variables in black box supervised learning models. *Journal of the Royal Statistical Society: Series B (Statistical Methodology)*. https://doi.org/10.1111/rssb.12377

Asad, A. L. (2020). On the Radar: System Embeddedness and Latin American Immigrants' Perceived Risk of Deportation. *Law & Society Review*, *54*(1), 133–167. https://doi.org/10.1111/lasr.12460

Bai, X., Ramos, M. R., & Fiske, S. T. (2020). As diversity increases, people paradoxically perceive social groups as more similar. *Proceedings of the National Academy of Sciences*, 202000333. https://doi.org/10.1073/pnas.2000333117

Bates, D. M., Mächler, M., Bolker, B., & Walker, S. (2015). Fitting linear mixed-effects models using lme4. *Journal of Statistical Software*, *67*(1), 1–48. https://doi.org/10.18637/jss.v067.i01

Berg, J. A. (2009). White Public Opinion toward Undocumented Immigrants: Threat and Interpersonal Environment. *Sociological Perspectives*, *52*(1), 39–58. https://doi.org/10.1525/sop.2009.52.1.39

Bobadilla-Suarez, S., Ahlheim, C., Mehrotra, A., Panos, A., & Love, B. C. (2018). Measures of neural similarity. *BioRxiv*. https://doi.org/10.1101/439893

Boutyline, A. (2017). Improving the Measurement of Shared Cultural Schemas with Correlational Class Analysis: Theory and Method. *Sociological Science*, *4*, 353–393. https://doi.org/10.15195/v4.a15

Bratko, I. (1997). Machine Learning: Between Accuracy and Interpretability. In G. Riccia, H.-J. Lenz, & R. Kruse (Eds.), *Learning, Networks and Statistics* (pp. 163–177). Springer Vienna. https://doi.org/10.1007/978-3-7091-2668-4_10

Breiman, L. (2001a). Random Forests. *Machine Learning*, *45*(1), 5–32. https://doi.org/10.1023/A:1010933404324

Breiman, L. (2001b). Statistical Modeling: The Two Cultures. *Statistical Science*, *16*(3), 199–231. https://doi.org/10.1214/ss/1009213726

Brinkman, L., Goffin, S., van de Schoot, R., van Haren, N. E. M., Dotsch, R., & Aarts, H. (2019). Quantifying the informational value of classification images. *Behavior Research Methods*, *51*(5), 2059–2073. https://doi.org/10.3758/s13428-019-01232-2

Brinkman, L., Todorov, A., & Dotsch, R. (2017). Visualising mental representations: A primer on noise-based reverse correlation in social psychology. *European Review of Social Psychology*, *28*(1), 333–361. https://doi.org/10.1080/10463283.2017.1381469

Chavez, L. R. (2013). *The Latino threat: Constructing immigrants, citizens, and the nation* (Second edition). Stanford University Press.

Chen, C., Liaw, A., & Breiman, L. (2004). *Using Random Forest to Learn Imbalanced Data*. 12.

Cikara, M. (2021). Causes and Consequences of Coalitional Cognition. *Advances in Experimental Social Psychology*, *64*, 65–128. https://doi.org/10.31219/osf.io/ktpf7

Cikara, M., Fouka, V., & Tabellini, M. (2022). Hate crime increases with minoritized group rank. *Nature Human Behaviour*. https://doi.org/10.1038/s41562-022-01416-5

Cikara, M., Martinez, J. E., & Lewis, N. A. (2022). Moving beyond social categories by incorporating context in social psychological theory. *Nature Reviews Psychology*. https://doi.org/10.1038/s44159-022-00079-3

Cone, J., Brown-Iannuzzi, J. L., Lei, R., & Dotsch, R. (2020). Type I Error Is Inflated in the Two-Phase Reverse Correlation Procedure. *Social Psychological and Personality Science*, 194855062093861. https://doi.org/10.1177/1948550620938616

Craig, M. A., & Richeson, J. A. (2018). Hispanic Population Growth Engenders Conservative Shift Among Non-Hispanic Racial Minorities. *Social Psychological and Personality Science*, *9*(4), 383–392. https://doi.org/10.1177/1948550617712029

Dalmaijer, E. S., Nord, C. L., & Astle, D. E. (2020). *Statistical power for cluster analysis*. https://doi.org/10.48550/ARXIV.2003.00381

Davis, J. T., & Perry, S. L. (2020). White Christian Nationalism and Relative Political Tolerance for Racists. *Social Problems*, spaa002. https://doi.org/10.1093/socpro/spaa002

DeBruine, L. (2020, January 31). *Composite Images*. Lisa DeBruine. https://debruine.github.io/post/composite-images/

DeBruine, L., & Jones, B. (2017). *Face Research Lab London Set* (p. 281699312 Bytes) [dataset]. figshare. https://doi.org/10.6084/M9.FIGSHARE.5047666.V3

Dotsch, R. (2017). *rcicr: Reverse correlation image classification toolbox.* (R package version 0.4.0) [Computer software].

Dotsch, R., Hassin, R. R., & Todorov, A. (2016). Statistical learning shapes face evaluation. *Nature Human Behaviour*, *1*(1), 1–6. https://doi.org/10.1038/s41562-016-0001

Dotsch, R., & Todorov, A. (2012). Reverse correlating social face perception. *Social Psychological and Personality Science*, *3*(5), 562–571. https://doi.org/10.1177/1948550611430272

Dotsch, R., Wigboldus, D. H. J., Langner, O., & van Knippenberg, A. (2008). Ethnic Out-Group Faces Are Biased in the Prejudiced Mind. *Psychological Science*, *19*(10), 978–980. https://doi.org/10.1111/j.1467-9280.2008.02186.x

Enos, R. D. (2017). *The space between us: Social geography and politics*. Cambridge University Press.

Everett, J. A. C. (2013). The 12 Item Social and Economic Conservatism Scale (SECS). *PLoS ONE*, *8*(12). https://doi.org/10.1371/journal.pone.0082131

Fields, K. E., & Fields, B. J. (2012). *Racecraft: The soul of inequality in American life*. Verso.

Filindra, A., & Kovács, M. (2012). Analysing US State Legislative Resolutions on Immigrants and Immigration: The Role of Immigration Federalism. *International Migration*, *50*(4), 33–50. https://doi.org/10.1111/j.1468-2435.2010.00658.x

Fisher, A. J., Medaglia, J. D., & Jeronimus, B. F. (2018). Lack of group-to-individual generalizability is a threat to human subjects research. *Proceedings of the National Academy of Sciences*, 201711978–201711978. https://doi.org/10.1073/pnas.1711978115

Griffith, B. (2021, March 22). *Map: Sanctuary Cities, Counties, and States*. CIS.Org. https://cis.org/Map-Sanctuary-Cities-Counties-and-States

Grigoropoulou, N., & Small, M. L. (2022). The data revolution in social science needs qualitative research. *Nature Human Behaviour*. https://doi.org/10.1038/s41562-022-01333-7

Hanel, P. H. P., Maio, G. R., & Manstead, A. S. R. (2019). A new way to look at the data: Similarities between groups of people are large and important. *Journal of Personality and Social Psychology*, *116*(4), 541–562. https://doi.org/10.1037/pspi0000154

Harrell, F. (2017, January 15). *Classification vs. Prediction*. Statistical Thinking. https://www.fharrell.com/post/classification/

Helms, J. E., Jernigan, M., & Mascher, J. (2005). The meaning of race in psychology and how to change it: A methodological perspective. *American Psychologist*, *60*(1), 27–36. https://doi.org/10.1037/0003-066X.60.1.27

Hinzman, L., & Maddox, K. B. (2017). Conceptual and visual representations of racial categories: Distinguishing subtypes from subgroups. *Journal of Experimental Social Psychology*, *70*, 95–109. https://doi.org/10.1016/j.jesp.2016.12.012

Hönekopp, J. (2006). Once more: Is beauty in the eye of the beholder? Relative contributions of private and shared taste to judgments of facial attractiveness. *Journal of Experimental Psychology. Human Perception and Performance*, *32*(2), 199–209. https://doi.org/10.1037/0096-1523.32.2.199

Hong, Y., & Ratner, K. G. (2020). Minimal but not meaningless: Seemingly arbitrary category labels can imply more than group membership. *Journal of Personality and Social Psychology*. https://doi.org/10.1037/pspa0000255

Hothorn, T., Hornik, K., & Zeileis, A. (2006). Unbiased Recursive Partitioning: A Conditional Inference Framework. *Journal of Computational and Graphical Statistics*, *15*(3), 651–674. https://doi.org/10.1198/106186006X133933

Huo, Y. J., Dovidio, J. F., Jiménez, T. R., & Schildkraut, D. J. (2018a). Local policy proposals can bridge Latino and (most) white Americans' response to immigration. *Proceedings of the National Academy of Sciences*, *115*(5), 945–950. https://doi.org/10.1073/pnas.1711293115

Huo, Y. J., Dovidio, J. F., Jiménez, T. R., & Schildkraut, D. J. (2018b). Not Just a National Issue: Effect of State-Level Reception of Immigrants and Population Changes on Intergroup Attitudes of Whites, Latinos, and Asians in the United States: Local Immigration Policy. *Journal of Social Issues*. https://doi.org/10.1111/josi.12295

Imhoff, R., Dotsch, R., Bianchi, M., Banse, R., & Wigboldus, D. H. J. (2011). Facing Europe: Visualizing spontaneous in-group projection. *Psychological Science*, *22*(12), 1583–1590. https://doi.org/10.1177/0956797611419675

Jones, Z., & Linder, F. (2015). *Exploratory Data Analysis using Random Forests*. 31.

Kahneman, D., Sibony, O., & Sunstein, C. R. (2021). *Noise: A flaw in human judgment*. Little, Brown and Company.

King, R. S. (2015). *Cluster analysis and data mining: An introduction*. Mercury Learning and Information.

Kriegeskorte. (2019, January 9). What's the best measure of representational dissimilarity? *Nikokriegeskorte*. https://nikokriegeskorte.org/2019/01/09/whats-the-best-measure-of-representational-dissimilarity/

Kriegeskorte, N., Mur, M., & Bandettini, P. (2008). Representational similarity analysis—Connecting the branches of systems neuroscience. *Frontiers in Systems Neuroscience*, *2*(November), 4–4. https://doi.org/10.3389/neuro.06.004.2008

Krosch, A. R., & Amodio, D. M. (2014). Economic scarcity alters the perception of race. *Proceedings of the National Academy of Sciences*, *111*(25), 9079–9084. https://doi.org/10.1073/pnas.1404448111

Kunst, J. R., Dovidio, J. F., & Thomsen, L. (2019). Fusion with political leaders predicts willingness to persecute immigrants and political opponents. *Nature Human Behaviour*. https://doi.org/10.1038/s41562-019-0708-1

Lei, R. F., & Bodenhausen, G. V. (2017). Racial assumptions color the mental representation of social class. *Frontiers in Psychology*, *8*(April), 1–7. https://doi.org/10.3389/fpsyg.2017.00519

Lenth, R. V. (2020). *emmeans: Estimated Marginal Means, aka Least-Squares Means.* (R package version 1.5.3) [Computer software]. https://github.com/rvlenth/emmeans

Luke, S. G. (2016). Evaluating significance in linear mixed-effects models in R. *Behavior Research Methods*, 1–9. https://doi.org/10.3758/s13428-016-0809-y

Martinez, J. E. (in press). Facecraft: Race reification in psychological research with faces. *Perspectives on Psychological Science*.

Martinez, J. E., Feldman, L. A., Feldman, M. J., & Cikara, M. (2021). Narratives shape cognitive representations of immigrants and immigration-policy preferences. *Psychological Science*, *32*(2), 135–152. https://doi.org/10.1177/0956797620963610

Martinez, J. E., Funk, F., & Todorov, A. (2020). Quantifying idiosyncratic and shared contributions to judgment. *Behavior Research Methods*, *52*(4), 1428–1444. https://doi.org/10.3758/s13428-019-01323-0

Martinez, J. E., Oh, D., & Todorov, A. (2021a). Immigrant faceism: Documentation statuses evoke racialized mental representations. *PsyArxiv*. https://doi.org/10.31234/osf.io/xb62n

Martinez, J. E., Oh, D., & Todorov, A. (2021b). Mental representations of immigrants encode racialized expectations of socio-structural positions. *PsyArxiv*. https://doi.org/10.31234/osf.io/cvhze

Martinez, J. E., & Paluck, E. L. (2020). Analytic racecraft: Race-based averages create illusory group differences in perceptions of racism. *PsyArxiv*. https://doi.org/10.31234/osf.io/kfpjg

Molnar, C. (2020). *Interpretable machine learning ; a guide for making black box models explainable*.

North, M. S. (2019). A GATE to Understanding "Older" Workers: Generation, Age, Tenure, Experience. *Academy of Management Annals*, *13*(2), 414–443. https://doi.org/10.5465/annals.2017.0125

Oh, D., Walker, M., & Freeman, J. B. (2021). Person knowledge shapes face identity perception. *Cognition*, *217*, 104889. https://doi.org/10.1016/j.cognition.2021.104889

Ommundsen, R., Larsen, K. S., van der Veer, K., & Eilertsen, D.-E. (2014). Framing Unauthorized Immigrants: The Effects of Labels on Evaluations. *Psychological Reports*, *114*(2), 461–478. https://doi.org/10.2466/17.PR0.114k20w0

Pew Research Center. (2019a). Metro area U.S. unauthorized immigrant population estimates, 2016 and 2007. *Pew Research Center's Hispanic Trends Project*. https://www.pewresearch.org/hispanic/interactives/unauthorized-immigrants-by-metro-area-table/

Pew Research Center. (2019b). U.S. unauthorized immigrant population estimates by state, 2016. *Pew Research Center's Hispanic Trends Project*. https://www.pewresearch.org/hispanic/interactives/u-s-unauthorized-immigrants-by-state/

Plascencia, L. F. B. (2009). The "Undocumented" Mexican Migrant Question: Re-Examining The Framing Of Law And Illegalization In The United States. *Urban Anthropology and Studies of Cultural Systems and World Economic Development*, *38*(2/3/4), 375–434.

Ramos, M. R., Bennett, M. R., Massey, D. S., & Hewstone, M. (2019). Humans adapt to social diversity over time. *Proceedings of the National Academy of Sciences*, *116*(25), 12244–12249. https://doi.org/10.1073/pnas.1818884116

Romero, M. (2006). Racial Profiling and Immigration Law Enforcement: Rounding Up of Usual Suspects in the Latino Community. *Critical Sociology*, *32*(2–3), 447–473. https://doi.org/10.1163/156916306777835376

Rosa, J. (2019). Contesting Representations of Migrant "Illegality" through the Drop the I-Word Campaign Rethinking Language Change and Social Change. In N. Avineri, L. R. Graham, E. J. Johnson, R. Conley Riner, & J. Rosa (Eds.), *Language and social justice in practice* (pp. 35–43). Routledge.

Rucker, J. M., Murphy, M. C., & Quintanilla, V. D. (2019). The immigrant labeling effect: The role of immigrant group labels in prejudice against noncitizens. *Group Processes & Intergroup Relations*, 136843021881874. https://doi.org/10.1177/1368430218818744

Sati, J. C. (2020). On Trumpism and Illegality. In O. K. Obasogie (Ed.), *Trumpism and its discontents* (pp. 115–129). Berkeley Public Policy Press.

Schönbrodt, F. D., & Perugini, M. (2013). At what sample size do correlations stabilize? *Journal of Research in Personality*, *47*(5), 609–612. https://doi.org/10.1016/j.jrp.2013.05.009

Sen, M., & Wasow, O. (2016). Race as a bundle of sticks: Designs that estimate effects of seemingly immutable characteristics. *Annual Review of Political Science*, *19*(1), 499–522. https://doi.org/10.1146/annurev-polisci-032015-010015

Sides, J., Tesler, M., & Vavreck, L. (2018). *Identity crisis: The 2016 presidential campaign and the battle for the meaning of America*. Princeton University Press.

Stephenson, W. (1935). Correlating persons instead of tests. *Journal of Personality*, *4*(1), 17–24. https://doi.org/10.1111/j.1467-6494.1935.tb02022.x

Tankard, M. E., & Paluck, E. L. (2016). Norm perception as a vehicle for social change. *Social Issues and Policy Review*, *10*(1), 181–211. https://doi.org/10.1111/sipr.12022

Todorov, A., & Oosterhof, N. N. (2011). Modeling social perception of faces. *Signal Processing Magazine, IEEE*, *28*, 117–122. https://doi.org/10.1109/MSP.2010.940006

Tosh, C., Greengard, P., Goodrich, B., Gelman, A., & Hsu, D. (2020). *The piranha problem: Large effects swimming in a small pond*.

Tucker, I. (2012). Deleuze, sense, and life: Marking the parameters of a psychology of individuation. *Theory & Psychology*, *22*(6), 771–785. https://doi.org/10.1177/0959354312442787

van Rijsbergen, N., Jaworska, K., Rousselet, G. A., & Schyns, P. G. (2014). With Age Comes Representational Wisdom in Social Signals. *Current Biology*, *24*(23), 2792–2796. https://doi.org/10.1016/j.cub.2014.09.075

Varsanyi, M. W., Lewis, P. G., Provine, D. M., & Decker, S. (2012). A Multilayered Jurisdictional Patchwork: Immigration Federalism in the United States: A MULTILAYERED JURISDICTIONAL PATCHWORK. *Law & Policy*, *34*(2), 138–158. https://doi.org/10.1111/j.1467-9930.2011.00356.x

Wang, D., & Liu, S. (2021). Doing Ethnography on Social Media: A Methodological Reflection on the Study of Online Groups in China. *Qualitative Inquiry*, 107780042110146. https://doi.org/10.1177/10778004211014610

Wang, N., Shi, W., Fan, C., & Zou, L. (2018). An improved nonlocal sparse regularization-based image deblurring via novel similarity criteria. *International Journal of Advanced Robotic Systems*, *15*(3), 172988141878311. https://doi.org/10.1177/1729881418783119

Wang, Z., Bovik, A. C., Sheikh, H. R., & Simoncelli, E. P. (2004). Image Quality Assessment: From Error Visibility to Structural Similarity. *IEEE Transactions on Image Processing*, *13*(4), 600–612. https://doi.org/10.1109/TIP.2003.819861

Watts, S., & Stenner, P. (2005). Doing Q methodology: Theory, method and interpretation. *Qualitative Research in Psychology*, *2*(1), 67–91. https://doi.org/10.1191/1478088705qp022oa

Wong, C. J. (2007). “Little” and “Big” Pictures in Our Heads: Race, Local Context, and Innumeracy About Racial Groups in the United States. *Public Opinion Quarterly*, *71*(3), 392–412. https://doi.org/10.1093/poq/nfm023

Wright, M. N., & Ziegler, A. (2017). ranger: A Fast Implementation of Random Forests for High Dimensional Data in C++ and R. *Journal of Statistical Software*, *77*(1). https://doi.org/10.18637/jss.v077.i01

Yim, O., & Ramdeen, K. T. (2015). Hierarchical Cluster Analysis: Comparison of Three Linkage Measures and Application to Psychological Data. *The Quantitative Methods for Psychology*, *11*(1), 8–21. https://doi.org/10.20982/tqmp.11.1.p008

Young, A. I., Ratner, K. G., & Fazio, R. H. (2014). Political Attitudes Bias the Mental Representation of a Presidential Candidate’s Face. *Psychological Science*, *25*(2), 503–510. https://doi.org/10.1177/0956797613510717

Zaller, J. (1992). *The nature and origins of mass opinion*. Cambridge University Press.

Mapping varied mental representations of illegalized immigrants -

Supplementary Material

Table of Contents:

- Table S1: Classification image generators' characteristics
- Table S2: Classification image raters' characteristics
- Figure S1: Google trends for labels across state and years
- Figure S2: Geographic map of sample based on IP addresses
- Figure S3: Correlation matrix of participant variables
- Figure S4: Agglomerative coefficient for different hierarchical clustering algorithms
- Figure S5: Maximum and minimum cluster size based on number of clusters and clustering algorithm
- Figure S6: Total within sums of squares (TWSS) across N cluster solutions
- Figure S7: Ten cluster solution from the hierarchical clustering analysis
- Figure S8: Permuted variable importance for ten cluster solution
- Figure S9: Partial dependence plots for ten cluster solution
- Figure S10: Fifteen cluster solution from the hierarchical clustering analysis
- Figure S11: Permuted variable importance for fifteen cluster solution
- Figure S12: Partial dependence plot for fifteen cluster solution
- Figure S13: Validation of random forest analysis and individual difference measures. The variable importance for individual difference predictors of support for building the Mexico-U.S. wall.
- Figure S14: Validation of random forest analysis and individual difference measures. Probabilistic responses of whether one agrees or disagrees strongly with building a Mexico-U.S. border wall across 2016 vote, political orientation, and political party.

Supplementary Table S1. Classification image generators' characteristics.

	California Illegal (N=250)	California Undocu (N=250)	Texas Illegal (N=252)	Texas Undocu (N=250)	Overall (N=1002)
Age					
Mean (SD)	37.4 (11.2)	38.7 (12.8)	38.3 (12.3)	37.7 (11.6)	38.0 (12.0)
Median [Min, Max]	35.0 [19.0, 72.0]	36.0 [18.0, 105]	35.0 [20.0, 73.0]	35.0 [19.0, 73.0]	35.0 [18.0, 105]
Gender Identity					
Agender	0 (0%)	0 (0%)	1 (0.4%)	0 (0%)	1 (0.1%)
Woman	132 (52.8%)	124 (49.6%)	144 (57.1%)	140 (56.0%)	540 (53.9%)
Man	114 (45.6%)	123 (49.2%)	106 (42.1%)	108 (43.2%)	451 (45.0%)
My gender is not listed	1 (0.4%)	0 (0%)	0 (0%)	0 (0%)	1 (0.1%)
Nonbinary	3 (1.2%)	3 (1.2%)	1 (0.4%)	2 (0.8%)	9 (0.9%)
Ethnoracial Background					
Black or African	27 (10.8%)	9 (3.6%)	43 (17.1%)	31 (12.4%)	110 (11.0%)
East Asian	32 (12.8%)	40 (16.0%)	9 (3.6%)	14 (5.6%)	95 (9.5%)
Hawaiian-Pacific Islander	4 (1.6%)	3 (1.2%)	0 (0%)	2 (0.8%)	9 (0.9%)
Indigenous-Native American	3 (1.2%)	0 (0%)	0 (0%)	0 (0%)	3 (0.3%)
Latinx-o-a or Hispanic	30 (12.0%)	46 (18.4%)	44 (17.5%)	40 (16.0%)	160 (16.0%)
Middle Eastern	0 (0%)	0 (0%)	1 (0.4%)	0 (0%)	1 (0.1%)
My race-ethnicity is not listed	12 (4.8%)	4 (1.6%)	2 (0.8%)	6 (2.4%)	24 (2.4%)
South Asian-Indian	8 (3.2%)	7 (2.8%)	5 (2.0%)	7 (2.8%)	27 (2.7%)
White or European	134 (53.6%)	141 (56.4%)	148 (58.7%)	150 (60.0%)	573 (57.2%)
Education Level					
Bachelors degree or similar	126 (50.4%)	117 (46.8%)	116 (46.0%)	104 (41.6%)	463 (46.2%)
High school or baccalaureate or A-levels	74 (29.6%)	67 (26.8%)	78 (31.0%)	91 (36.4%)	310 (30.9%)
I did not complete secondary-high school	0 (0%)	2 (0.8%)	1 (0.4%)	1 (0.4%)	4 (0.4%)
Masters or Doctoral degree	31 (12.4%)	40 (16.0%)	23 (9.1%)	31 (12.4%)	125 (12.5%)
Professional qualification	19 (7.6%)	24 (9.6%)	34 (13.5%)	23 (9.2%)	100 (10.0%)
Religious Affiliation					

	California Illegal (N=250)	California Undocu (N=250)	Texas Illegal (N=252)	Texas Undocu (N=250)	Overall (N=1002)
Agnostic	43 (17.2%)	42 (16.8%)	25 (9.9%)	33 (13.2%)	143 (14.3%)
Atheist	32 (12.8%)	32 (12.8%)	39 (15.5%)	24 (9.6%)	127 (12.7%)
Buddhist	4 (1.6%)	8 (3.2%)	3 (1.2%)	7 (2.8%)	22 (2.2%)
Hindu	2 (0.8%)	2 (0.8%)	2 (0.8%)	3 (1.2%)	9 (0.9%)
Jewish	2 (0.8%)	8 (3.2%)	3 (1.2%)	4 (1.6%)	17 (1.7%)
Mormon	3 (1.2%)	3 (1.2%)	1 (0.4%)	0 (0%)	7 (0.7%)
Muslim	4 (1.6%)	3 (1.2%)	4 (1.6%)	1 (0.4%)	12 (1.2%)
My religion is not listed	19 (7.6%)	11 (4.4%)	22 (8.7%)	31 (12.4%)	83 (8.3%)
Nothing in particular	53 (21.2%)	40 (16.0%)	41 (16.3%)	48 (19.2%)	182 (18.2%)
Orthodox such as Greek or Russian Orthodox	3 (1.2%)	0 (0%)	1 (0.4%)	0 (0%)	4 (0.4%)
Protestant	48 (19.2%)	49 (19.6%)	60 (23.8%)	55 (22.0%)	212 (21.2%)
Roman Catholic	37 (14.8%)	52 (20.8%)	51 (20.2%)	44 (17.6%)	184 (18.4%)
Born in U.S.					
No	19 (7.6%)	23 (9.2%)	18 (7.1%)	14 (5.6%)	74 (7.4%)
Yes	231 (92.4%)	227 (90.8%)	234 (92.9%)	236 (94.4%)	928 (92.6%)
U.S. Citizen					
No	2 (0.8%)	4 (1.6%)	6 (2.4%)	6 (2.4%)	18 (1.8%)
Prefer not to say	3 (1.2%)	1 (0.4%)	0 (0%)	0 (0%)	4 (0.4%)
Yes	245 (98.0%)	245 (98.0%)	246 (97.6%)	244 (97.6%)	980 (97.8%)
Immigrant Contact					
Mean (SD)	3.32 (1.88)	3.32 (1.85)	2.91 (1.89)	3.18 (1.95)	3.18 (1.90)
Median [Min, Max]	4.00 [0, 5.00]	4.00 [0, 5.00]	3.00 [0, 5.00]	4.00 [0, 5.00]	3.00 [0, 5.00]
Estimated immigrant pop. in neighborhood					
Mean (SD)	12.7 (14.0)	12.3 (13.6)	12.5 (15.1)	12.4 (15.3)	12.5 (14.5)
Median [Min, Max]	9.00 [0, 60.0]	6.00 [0, 60.0]	5.00 [0, 60.0]	5.00 [0, 60.0]	5.00 [0, 60.0]
Estimated immigrant pop. in city					

	California Illegal (N=250)	California Undocu (N=250)	Texas Illegal (N=252)	Texas Undocu (N=250)	Overall (N=1002)
Mean (SD)	18.8 (14.8)	18.3 (14.3)	19.3 (16.3)	19.7 (15.5)	19.0 (15.2)
Median [Min, Max]	15.0 [0, 60.0]	15.0 [1.00, 60.0]	15.0 [0, 60.0]	16.0 [0, 60.0]	15.0 [0, 60.0]
Estimated immigrant pop. in state					
Mean (SD)	24.3 (14.8)	23.4 (13.6)	24.4 (15.3)	26.3 (16.3)	24.6 (15.1)
Median [Min, Max]	22.0 [0, 60.0]	21.0 [2.00, 60.0]	21.0 [0, 60.0]	21.0 [2.00, 60.0]	21.0 [0, 60.0]
Illegal Immigrant Scale					
Mean (SD)	3.00 (0.297)	2.99 (0.307)	2.99 (0.315)	3.00 (0.300)	3.00 (0.304)
Median [Min, Max]	3.00 [2.05, 4.35]	3.00 [2.15, 4.20]	3.00 [1.80, 3.90]	3.05 [2.00, 3.85]	3.00 [1.80, 4.35]
Conservatism					
Mean (SD)	58.0 (17.5)	59.2 (17.2)	59.9 (17.7)	61.1 (17.0)	59.5 (17.4)
Median [Min, Max]	58.8 [14.8, 95.8]	60.0 [10.9, 98.3]	61.3 [8.25, 95.8]	63.2 [16.0, 95.4]	60.5 [8.25, 98.3]
Build the wall?					
Missing response	3 (1.2%)	2 (0.8%)	5 (2.0%)	1 (0.4%)	11 (1.1%)
Agree	24 (9.6%)	28 (11.2%)	33 (13.1%)	41 (16.4%)	126 (12.6%)
Agree Strongly	35 (14.0%)	41 (16.4%)	44 (17.5%)	41 (16.4%)	161 (16.1%)
Disagree	49 (19.6%)	42 (16.8%)	42 (16.7%)	44 (17.6%)	177 (17.7%)
Disagree Strongly	112 (44.8%)	106 (42.4%)	97 (38.5%)	90 (36.0%)	405 (40.4%)
Undecided	27 (10.8%)	31 (12.4%)	31 (12.3%)	33 (13.2%)	122 (12.2%)
Vote in 2016					
Chose not to vote	48 (19.2%)	45 (18.0%)	59 (23.4%)	63 (25.2%)	215 (21.5%)
Could not vote	9 (3.6%)	12 (4.8%)	17 (6.7%)	14 (5.6%)	52 (5.2%)
Donald Trump & Mike Pence, Republican Party	46 (18.4%)	54 (21.6%)	71 (28.2%)	71 (28.4%)	242 (24.2%)
Gary Johnson & Bill Weld, Libertarian Party	5 (2.0%)	18 (7.2%)	5 (2.0%)	7 (2.8%)	35 (3.5%)
Hillary Clinton & Tim Kaine, Democratic Party	118 (47.2%)	108 (43.2%)	89 (35.3%)	80 (32.0%)	395 (39.4%)

	California Illegal (N=250)	California Undocu (N=250)	Texas Illegal (N=252)	Texas Undocu (N=250)	Overall (N=1002)
Jill Stein & Ajamu Baraka, Green Party	8 (3.2%)	5 (2.0%)	3 (1.2%)	5 (2.0%)	21 (2.1%)
Other Candidate	16 (6.4%)	8 (3.2%)	8 (3.2%)	10 (4.0%)	42 (4.2%)
Political Party Affiliation					
Democrat	125 (50.0%)	109 (43.6%)	99 (39.3%)	90 (36.0%)	423 (42.2%)
Green	4 (1.6%)	3 (1.2%)	1 (0.4%)	0 (0%)	8 (0.8%)
Independent	54 (21.6%)	53 (21.2%)	53 (21.0%)	62 (24.8%)	222 (22.2%)
Libertarian	5 (2.0%)	9 (3.6%)	5 (2.0%)	6 (2.4%)	25 (2.5%)
Republican	39 (15.6%)	56 (22.4%)	67 (26.6%)	59 (23.6%)	221 (22.1%)
Unaffiliated/Not political	23 (9.2%)	20 (8.0%)	27 (10.7%)	33 (13.2%)	103 (10.3%)
Self-report state					
Arizona	0 (0%)	1 (0.4%)	3 (1.2%)	0 (0%)	4 (0.4%)
Arkansas	1 (0.4%)	0 (0%)	0 (0%)	0 (0%)	1 (0.1%)
California	247 (98.8%)	248 (99.2%)	1 (0.4%)	0 (0%)	496 (49.5%)
Colorado	1 (0.4%)	0 (0%)	0 (0%)	0 (0%)	1 (0.1%)
Illinois	0 (0%)	0 (0%)	1 (0.4%)	0 (0%)	1 (0.1%)
Iowa	1 (0.4%)	0 (0%)	0 (0%)	0 (0%)	1 (0.1%)
Louisiana	0 (0%)	0 (0%)	1 (0.4%)	0 (0%)	1 (0.1%)
Missouri	0 (0%)	0 (0%)	1 (0.4%)	1 (0.4%)	2 (0.2%)
New York	0 (0%)	1 (0.4%)	0 (0%)	0 (0%)	1 (0.1%)
Oklahoma	0 (0%)	0 (0%)	0 (0%)	1 (0.4%)	1 (0.1%)
Texas	0 (0%)	0 (0%)	244 (96.8%)	248 (99.2%)	492 (49.1%)
Washington D.C.	0 (0%)	0 (0%)	1 (0.4%)	0 (0%)	1 (0.1%)
State from IP address					
Arizona	0 (0%)	1 (0.4%)	0 (0%)	0 (0%)	1 (0.1%)
Arkansas	0 (0%)	0 (0%)	1 (0.4%)	0 (0%)	1 (0.1%)
California	248 (99.2%)	246 (98.4%)	0 (0%)	0 (0%)	494 (49.3%)
New Mexico	0 (0%)	0 (0%)	0 (0%)	1 (0.4%)	1 (0.1%)
North Carolina	0 (0%)	1 (0.4%)	0 (0%)	0 (0%)	1 (0.1%)
Texas	0 (0%)	0 (0%)	247	247	494

	California Illegal (N=250)	California Undocu (N=250)	Texas Illegal (N=252)	Texas Undocu (N=250)	Overall (N=1002)
			(98.0%)	(98.8%)	(49.3%)
Missing	2 (0.8%)	2 (0.8%)	4 (1.6%)	2 (0.8%)	10 (1.0%)
How long lived in state?					
Less than 1 month	1 (0.4%)	0 (0%)	3 (1.2%)	2 (0.8%)	6 (0.6%)
Less than 1 year	0 (0%)	2 (0.8%)	4 (1.6%)	1 (0.4%)	7 (0.7%)
Over 1 year	20 (8.0%)	22 (8.8%)	24 (9.5%)	21 (8.4%)	87 (8.7%)
Over 10 years	229 (91.6%)	226 (90.4%)	221 (87.7%)	226 (90.4%)	902 (90.0%)
Image Informational Value					
Mean (SD)	0.644 (1.37)	0.635 (1.41)	0.663 (1.44)	0.612 (1.35)	0.639 (1.39)
Median [Min, Max]	0.543 [-2.16, 7.18]	0.444 [-2.40, 7.59]	0.427 [-2.38, 8.43]	0.542 [-2.15, 5.14]	0.478 [-2.40, 8.43]

Table S2: Classification image raters' characteristics.

	Dangerous (N=46)	Dominant (N=44)	American (N=46)	Ethnoracial Category (N=87)	Overall (N=223)
Age					
Mean (SD)	38.3 (10.4)	36.9 (12.0)	40.2 (12.9)	38.1 (12.4)	38.3 (12.0)
Median [Min, Max]	36.0 [25.0, 69.0]	33.5 [20.0, 72.0]	36.5 [20.0, 73.0]	35.0 [21.0, 68.0]	35.0 [20.0, 73.0]
Gender					
Man	32 (69.6%)	25 (56.8%)	24 (52.2%)	54 (62.1%)	135 (60.5%)
Woman	14 (30.4%)	19 (43.2%)	22 (47.8%)	33 (37.9%)	88 (39.5%)
Race					
Black or African	4 (8.7%)	12 (27.3%)	5 (10.9%)	12 (13.8%)	33 (14.8%)
East Asian	3 (6.5%)	2 (4.5%)	3 (6.5%)	3 (3.4%)	11 (4.9%)
Latinx/o/a or Hispanic	3 (6.5%)	2 (4.5%)	1 (2.2%)	4 (4.6%)	10 (4.5%)
White or European	36 (78.3%)	27 (61.4%)	36 (78.3%)	63 (72.4%)	162 (72.6%)
Indigenous/Native American	0 (0%)	1 (2.3%)	0 (0%)	0 (0%)	1 (0.4%)
South Asian/Indian	0 (0%)	0 (0%)	1 (2.2%)	3 (3.4%)	4 (1.8%)
My race/ethnicity is not listed	0 (0%)	0 (0%)	0 (0%)	2 (2.3%)	2 (0.9%)
Born in U.S.					
No	1 (2.2%)	2 (4.5%)	1 (2.2%)	5 (5.7%)	9 (4.0%)
Yes	45 (97.8%)	42 (95.5%)	45 (97.8%)	82 (94.3%)	214 (96.0%)
Social and Economic Conservatism Scale					
Mean (SD)	58.4 (19.7)	60.3 (19.8)	58.4 (19.4)	58.8 (21.6)	58.9 (20.3)

	Dangerous (N=46)	Dominant (N=44)	American (N=46)	Ethnoracial Category (N=87)	Overall (N=223)
Median [Min, Max]	59.0 [19.1, 94.9]	64.5 [16.0, 90.4]	54.8 [15.4, 91.6]	59.0 [15.5, 100]	60.5 [15.4, 100]
Test-Retest Reliability					
Mean (SD)	0.352 (0.213)	0.296 (0.242)	0.373 (0.201)	0.471 (0.233)	0.391 (0.233)
Median [Min, Max]	0.380 [0.00673, 0.752]	0.250 [0.0108, 0.780]	0.363 [0.0548, 0.849]	0.501 [0.0135, 0.894]	0.407 [0.00673, 0.894]

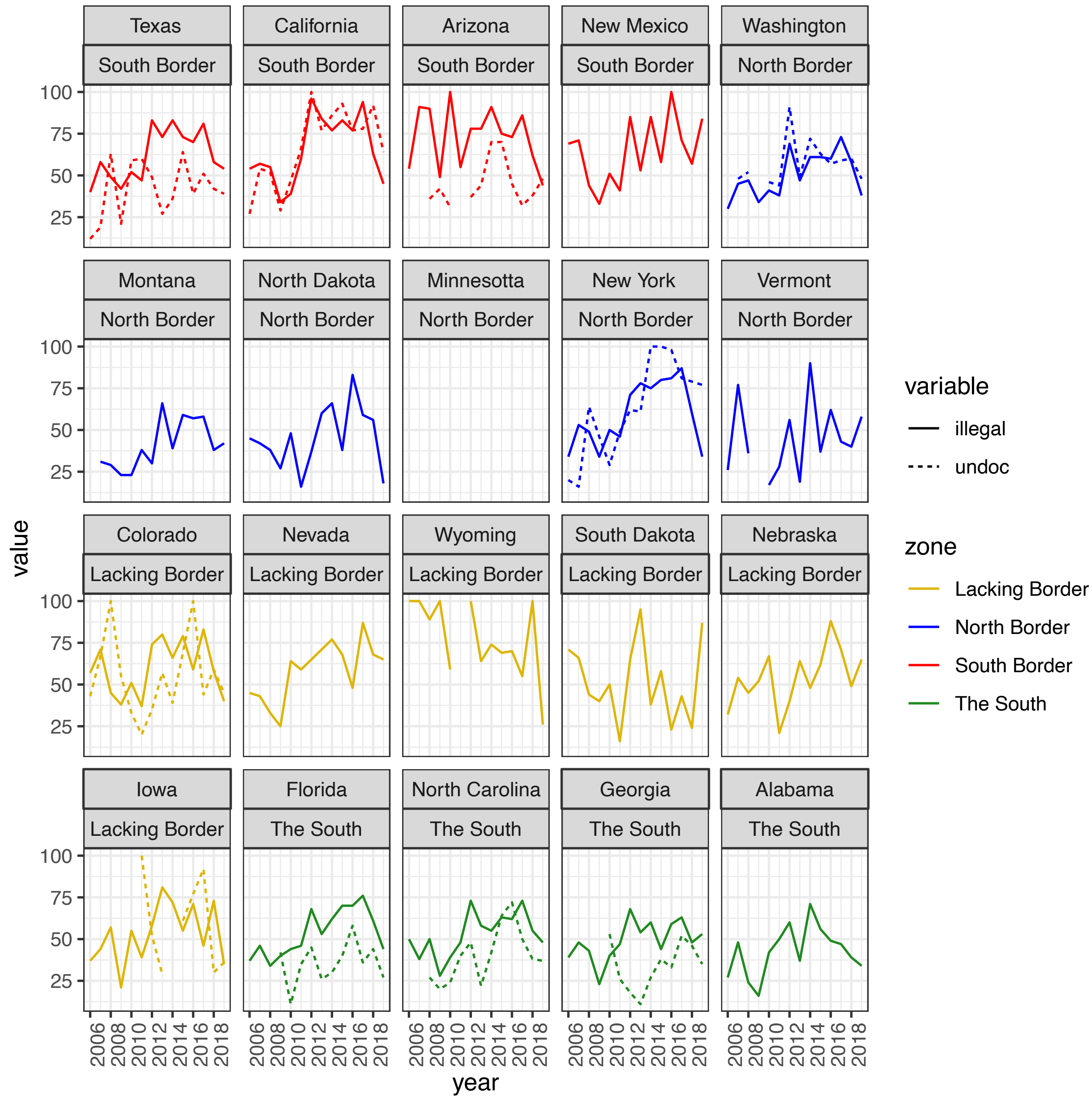

Supplementary Figure S1. Google trends for labels across state and years. Each plot represents a different state that was under consideration in the design of this study before settling on Texas and California. States are color coded by zones considered to have different relationships to migration based on distance to a border or historical migration patterns. The solid line is for "illegal immigrant" searches, the dotted line is for "undocumented immigrant" searches. Missing lines suggest data were unavailable for those time periods or states. The x-axis is year (2006 to 2019) in which the label searches occurred and the y-axis is a normalized value that represents the number of searches as a proportion of all searches in the same time period and region. It can be interpreted as public interest.

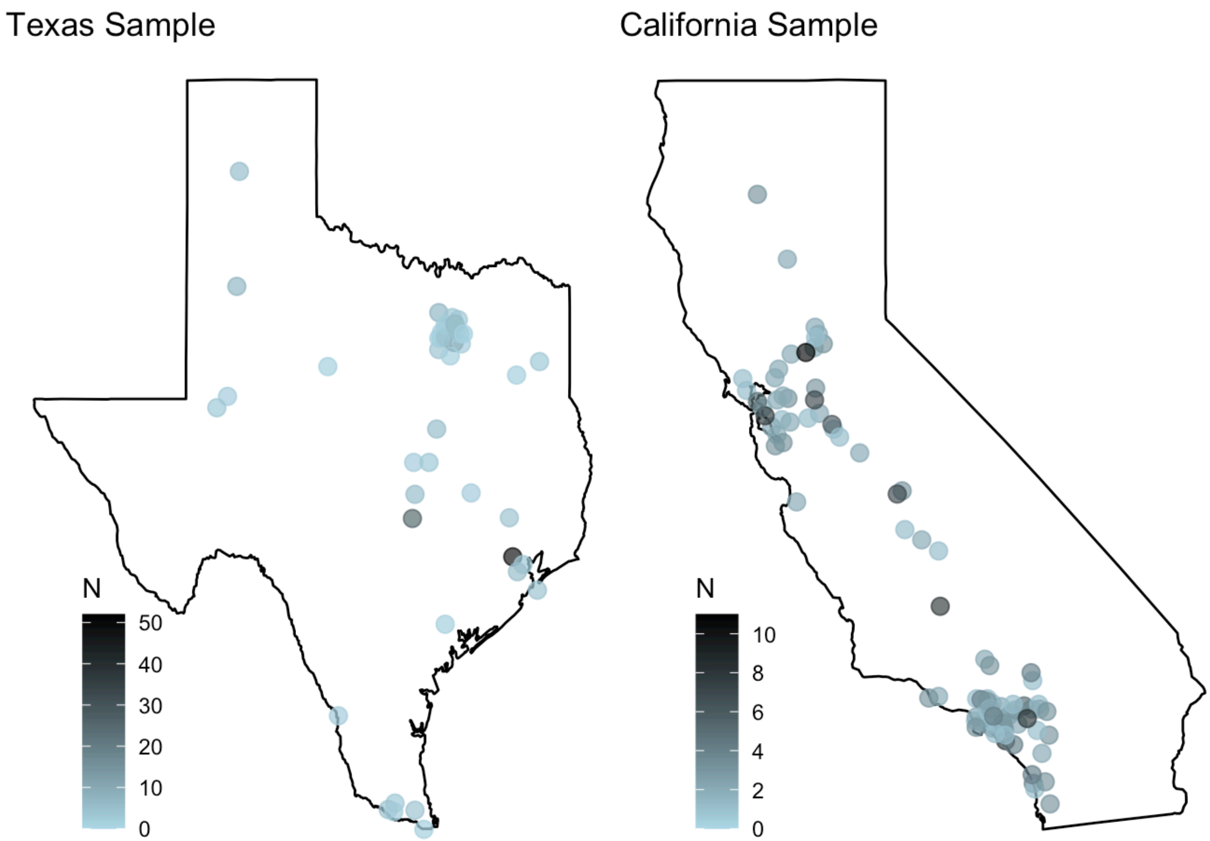

Supplementary Figure S2. Geographic map of sample based on IP addresses. Left panel represents participants from Texas, right panel from California. The location of the dots represents various cities and the color of the dot is the number of participants in each city where darker colors represent more participants. Texas had more representation from metropolitan areas: Houston, Dallas-Fort Worth, Austin, Brownsville. California had more representation from the Bay Area (e.g., San Francisco) and southern Californian areas around Los Angeles and San Diego.

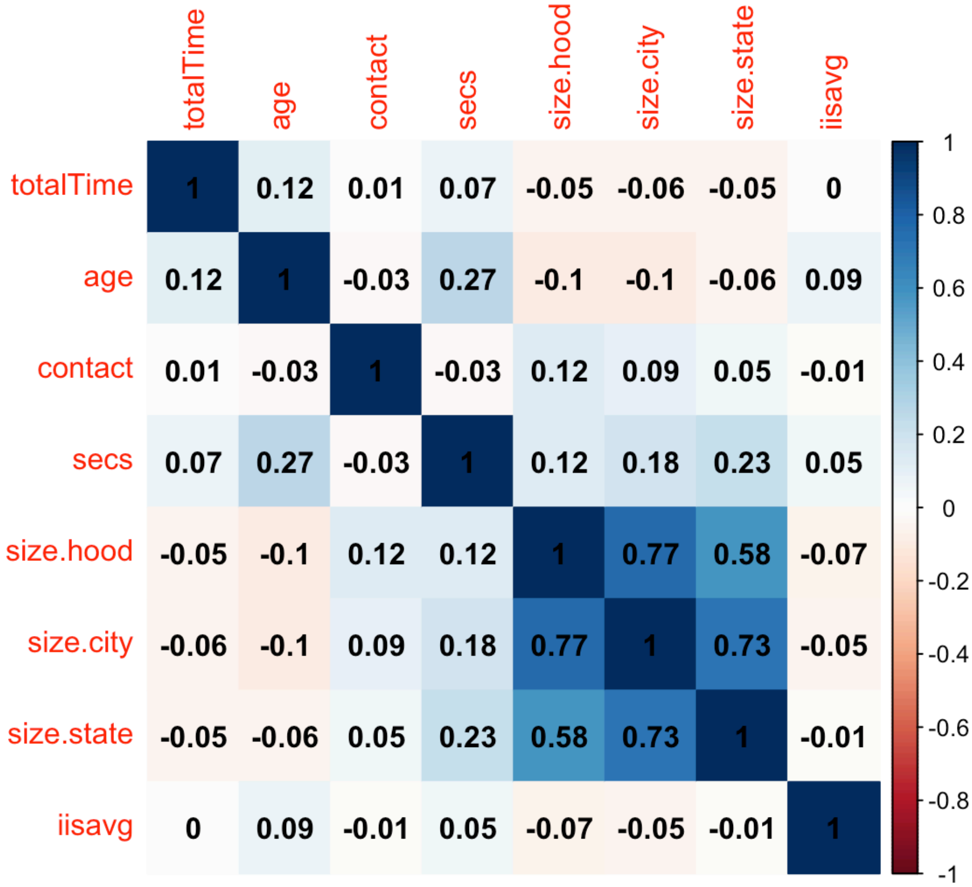

Supplementary Figure S3. Correlation matrix of participant variables. Cooler colors represent positively correlated variables, hotter colors represent negatively correlated variables. Variable order from top to bottom (or left to right): time on task, age, immigrant contact, social and economic conservatism, estimated immigrant population size in neighborhood, in city, in state, illegal immigrant scale average score. Note: "size" is the estimated size of the surrounding undocumented population, "hood" is neighborhood, "secs" is the political orientation scale, "iiasvg" is the illegal immigration attitude scale, and "totalTime" was the completion duration for the task.

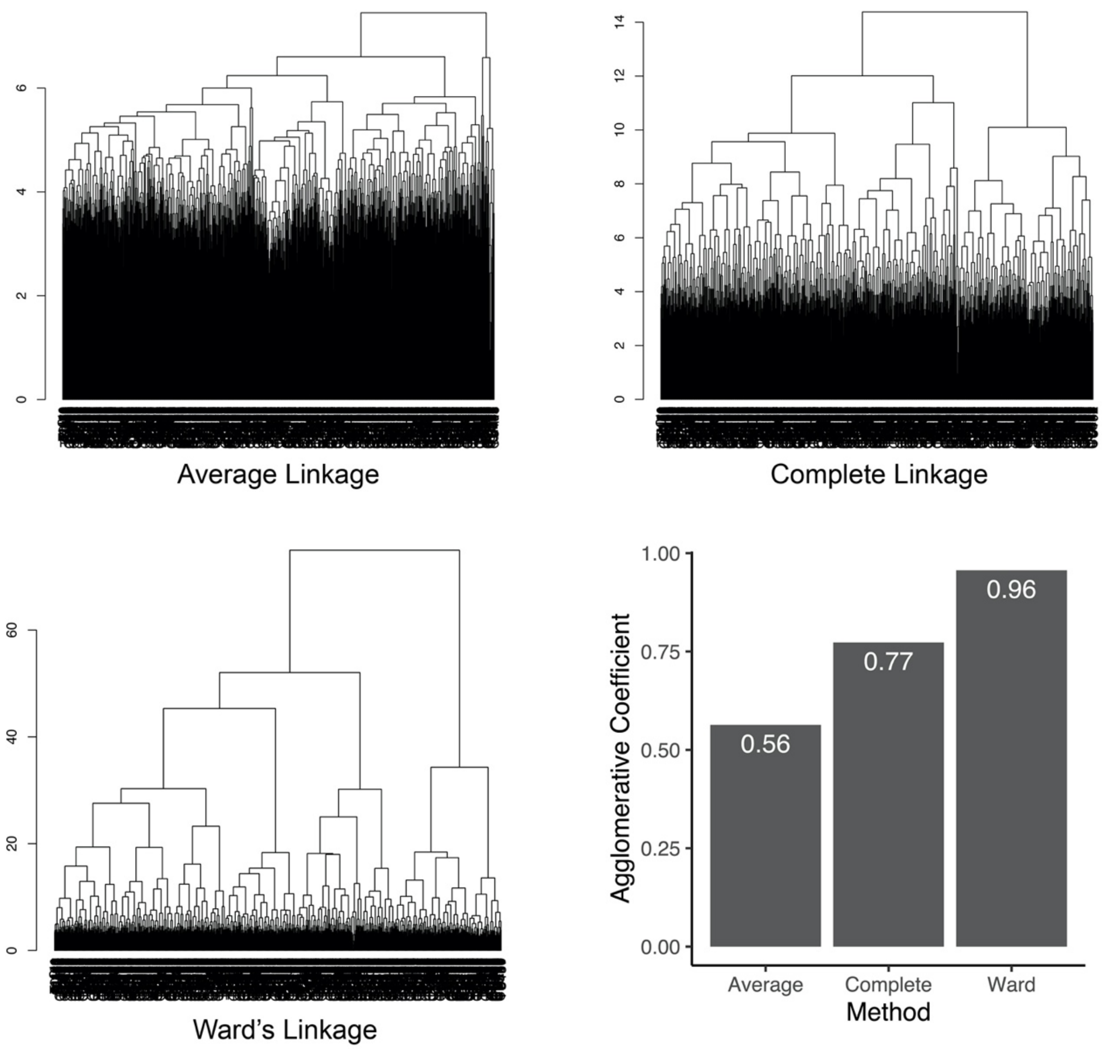

Supplementary Figure S4. Agglomerative coefficient for different hierarchical clustering algorithms. The top panels and bottom left panel are the dendrograms for the various similarity linkage algorithms. The bottom right panel depicts the agglomerative coefficient for the various linkage algorithms. There is a clearer cluster structure in the Ward dendrogram than the other linkages, as reflected in the higher agglomerative coefficient.

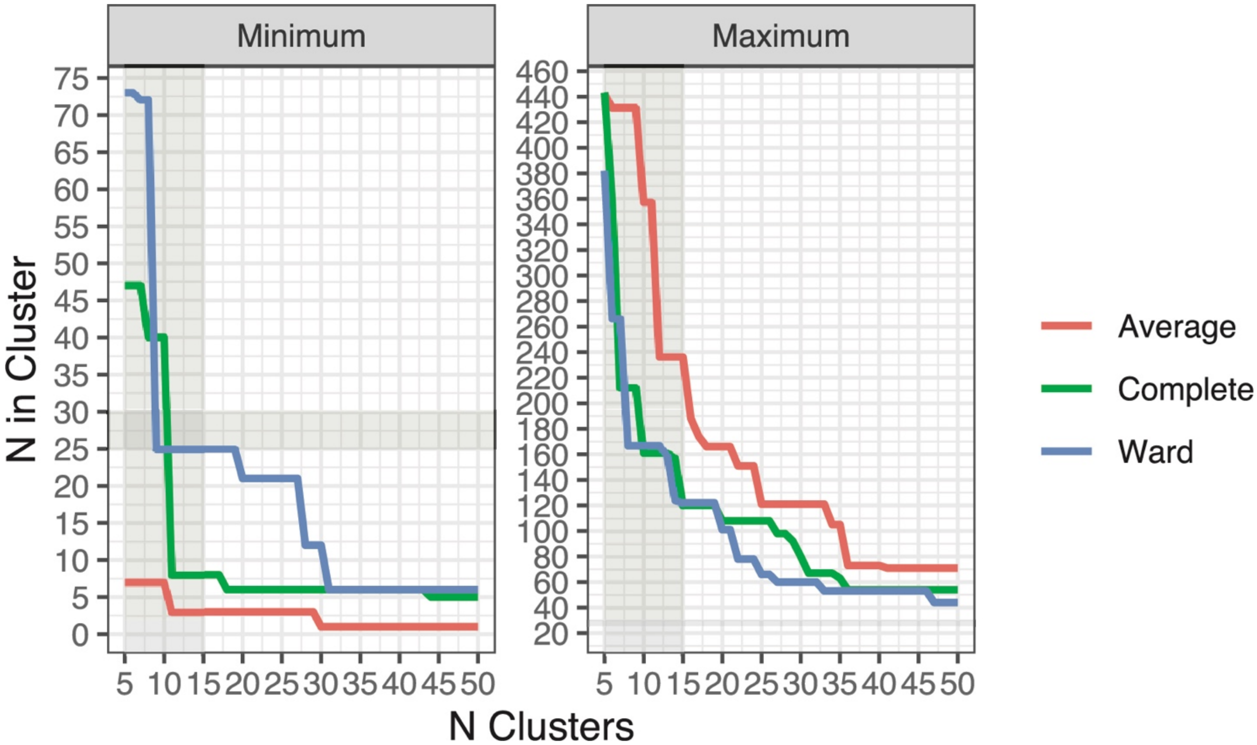

Supplementary Figure S5. Maximum and minimum cluster size based on number of clusters and clustering algorithm. The left panel shows the minimum sample size across the clusters at various N cluster solutions. The colors represent the linkage algorithms. The y-axis is the sample size of the smallest cluster at each solution. The right panel depicts the largest or maximum sample size at each cluster solution. The 5-15 range which was chosen for the study is highlighted in grey.

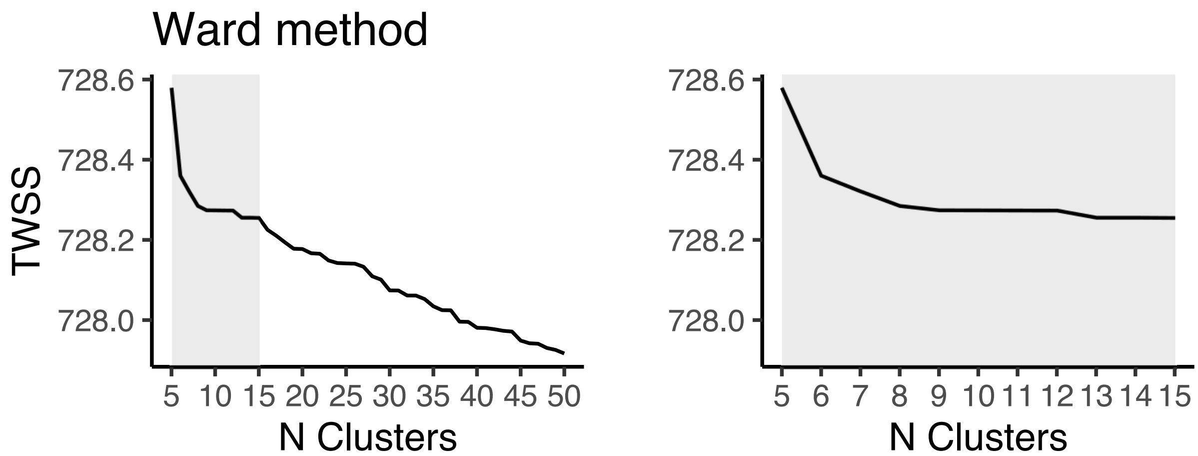

Supplementary Figure S6. Total within sums of squares (TWSS) across N cluster solutions. The left panel depicts the TWSS values (y-axis) across different number of cluster solutions (x-axis). The right panel zooms in on the 5-15 cluster range. There is a leveling off at the 7 cluster area. After 15 clusters, there is a decrease. However, interpreting more than 15 face clusters is very difficult, so we focused on the restricted range of 5-15 clusters.

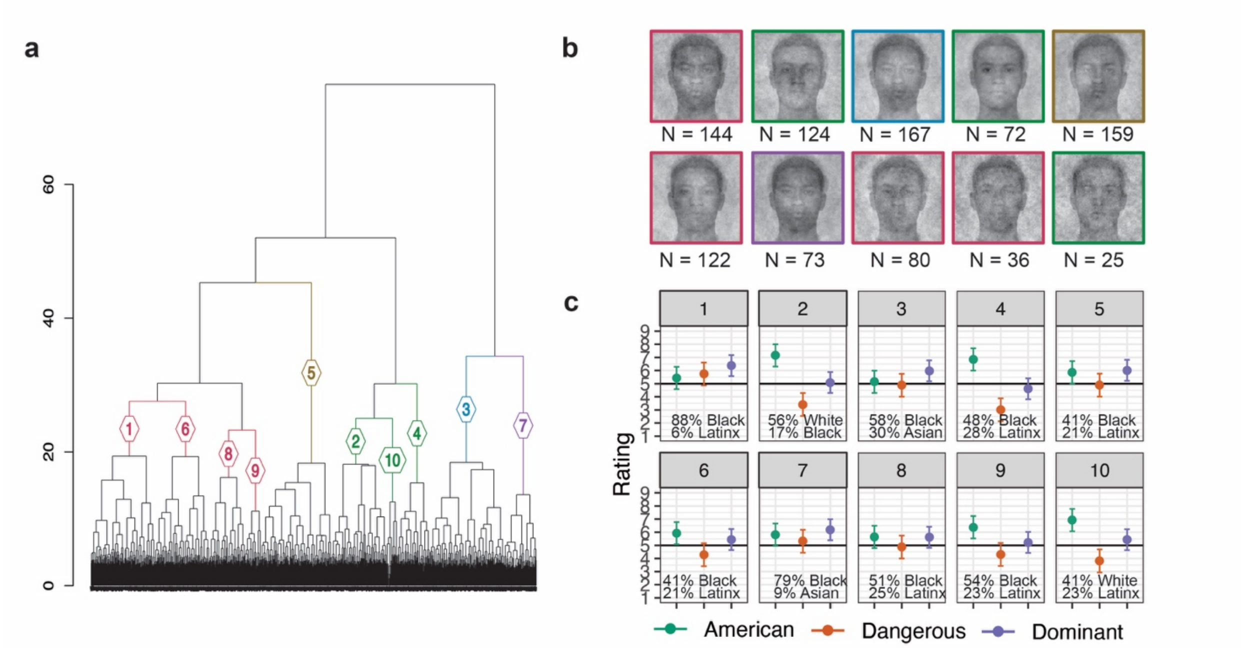

Supplementary Figure S7. Ten cluster solution from the hierarchical clustering analysis. a. Dendrogram depicting the ten clusters in the same colors as Figure 2 (e.g., cluster 1 is broken down into clusters 1, 6, 8, 9 all in red). **b.** The average faces and sample sizes from each cluster (color coded to match the dendrogram). **c.** The estimated marginal means from the trait ratings for each face. The error bars depict 95% confidence intervals. The horizontal line is the neutral scale position of each rating. The percentages reflect the top two ethnoracial classifications.

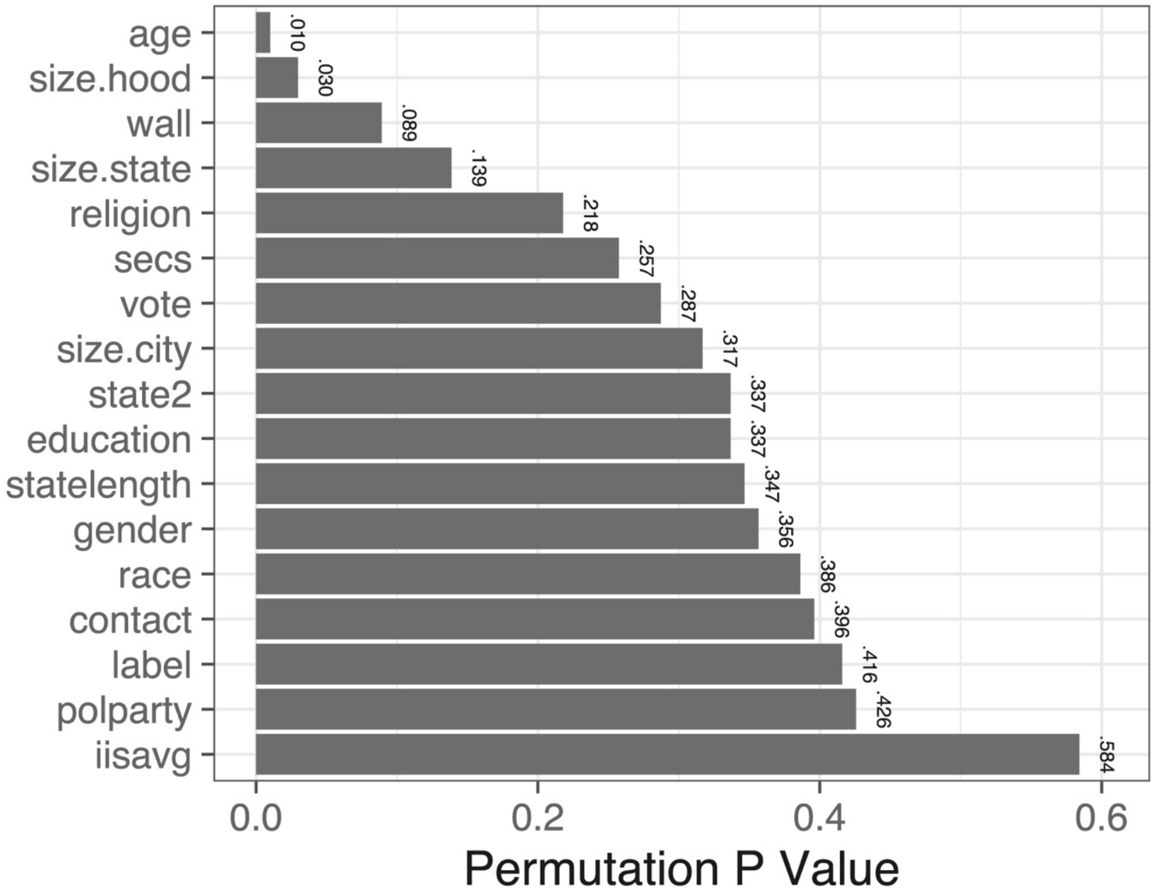

Supplementary Figure S8. Permuted variable importance for ten cluster solution. The x-axis is the permuted p value representing variable importance (significant alpha is .05). The exact p value is provided to the right of each bar. The y-axis lists all the individual difference measures.

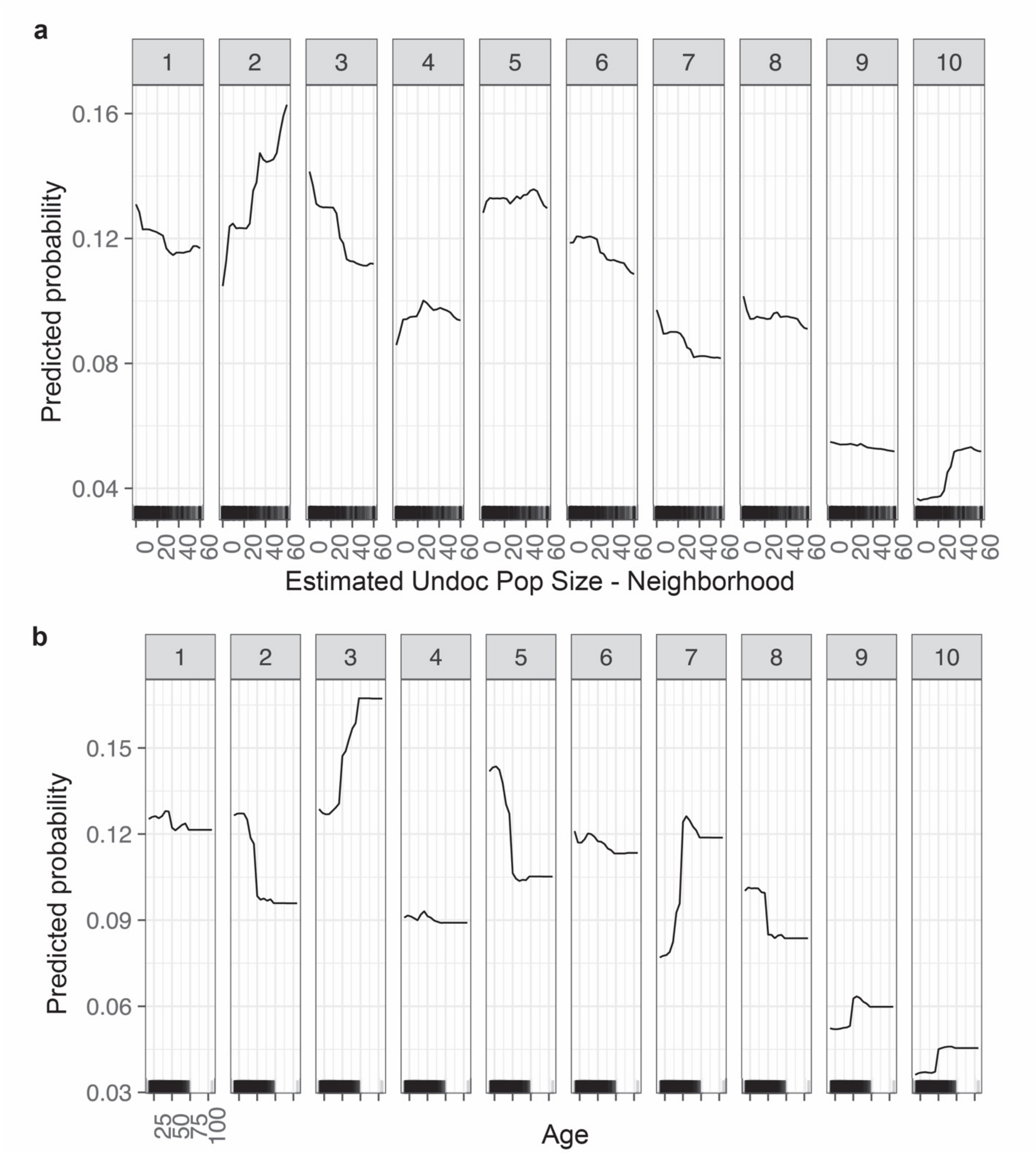

Supplementary Figure S9. Partial dependence plots for ten cluster solution. a. Probabilistic cluster membership across undocumented population size in the neighborhood. **b.** Estimates across age. The y-axis is the probability of cluster membership. The black tick marks above the x-axis are data points such that the less tick marks the less participants at that level of the x-axis variable.

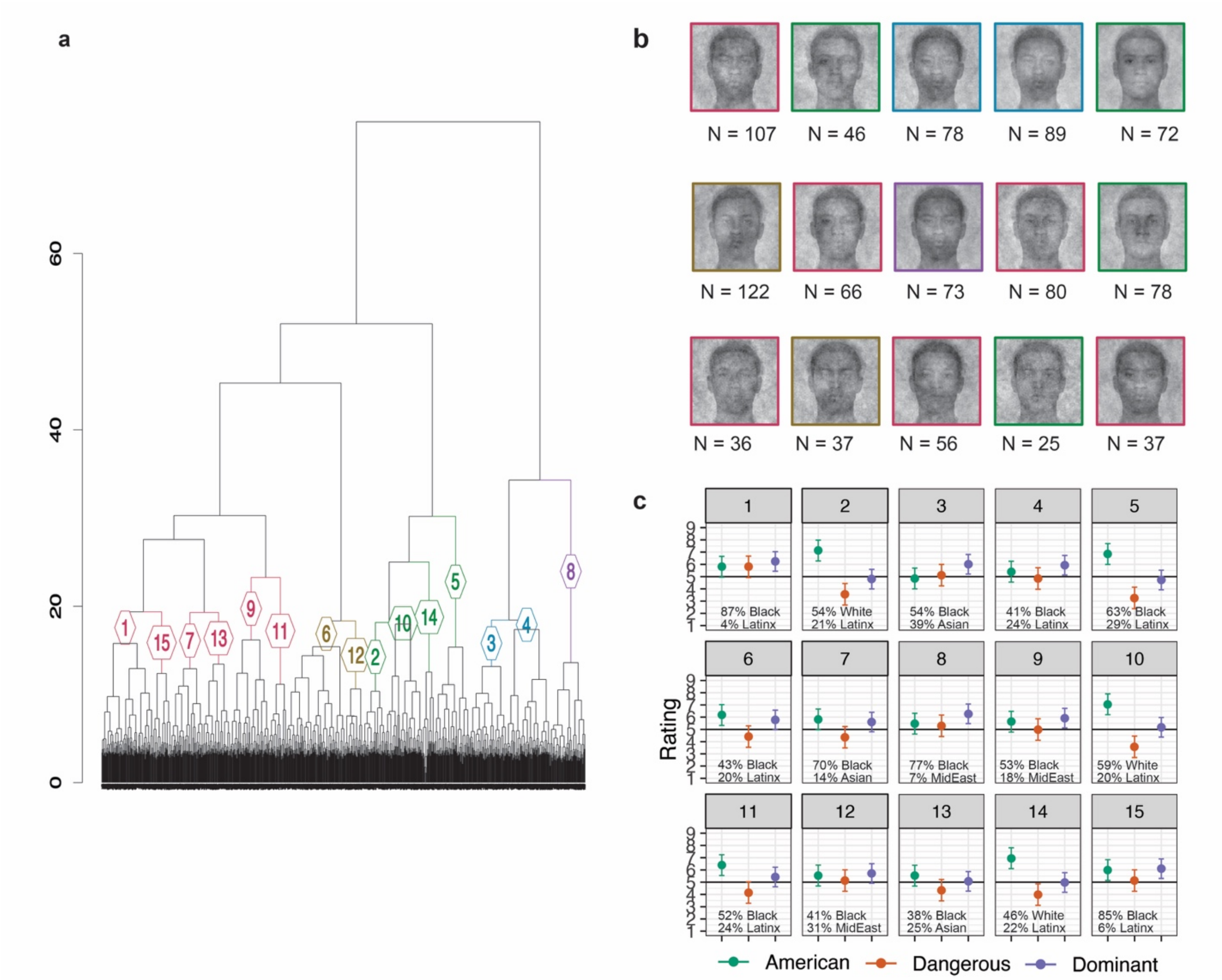

Supplementary Figure S10. Fifteen cluster solution from the hierarchical clustering analysis. a. Dendrogram depicting the fifteen clusters in the same colors as Figure 2 (e.g., Cluster 1 is broken down into clusters 1, 15, 7, 13, 9, 11 all in red). **b.** The average faces and sample sizes from each cluster (color coded to match the dendrogram). **c.** The estimated marginal means from the trait ratings for each face. The error bars depict 95% confidence intervals. The horizontal line is the neutral scale position of each rating. The percentages reflect the top two ethnoracial classifications.

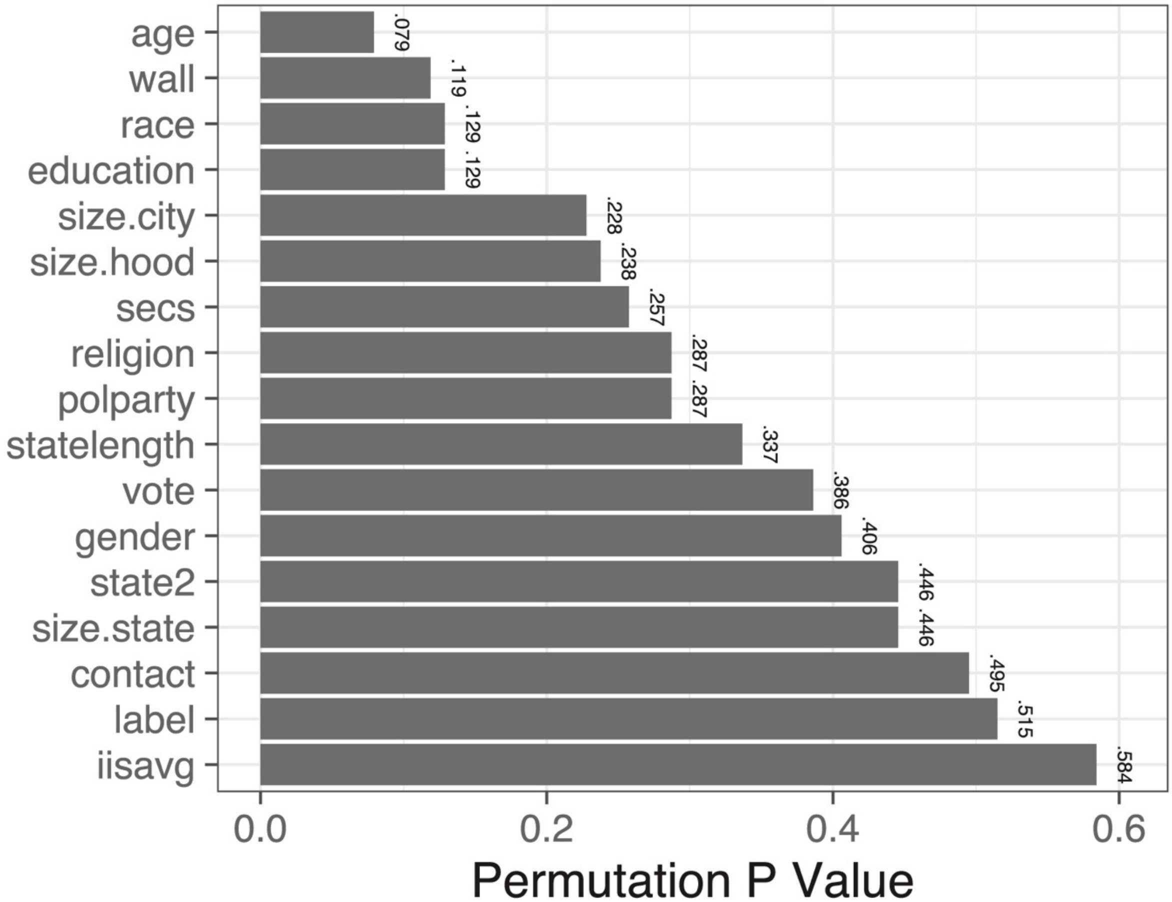

Supplementary Figure S11. Permuted variable importance for fifteen cluster solution. The x-axis is the permuted p value representing variable importance (significant alpha is .05). The exact p value is provided to the right of each bar. The y-axis lists all the individual difference measures.

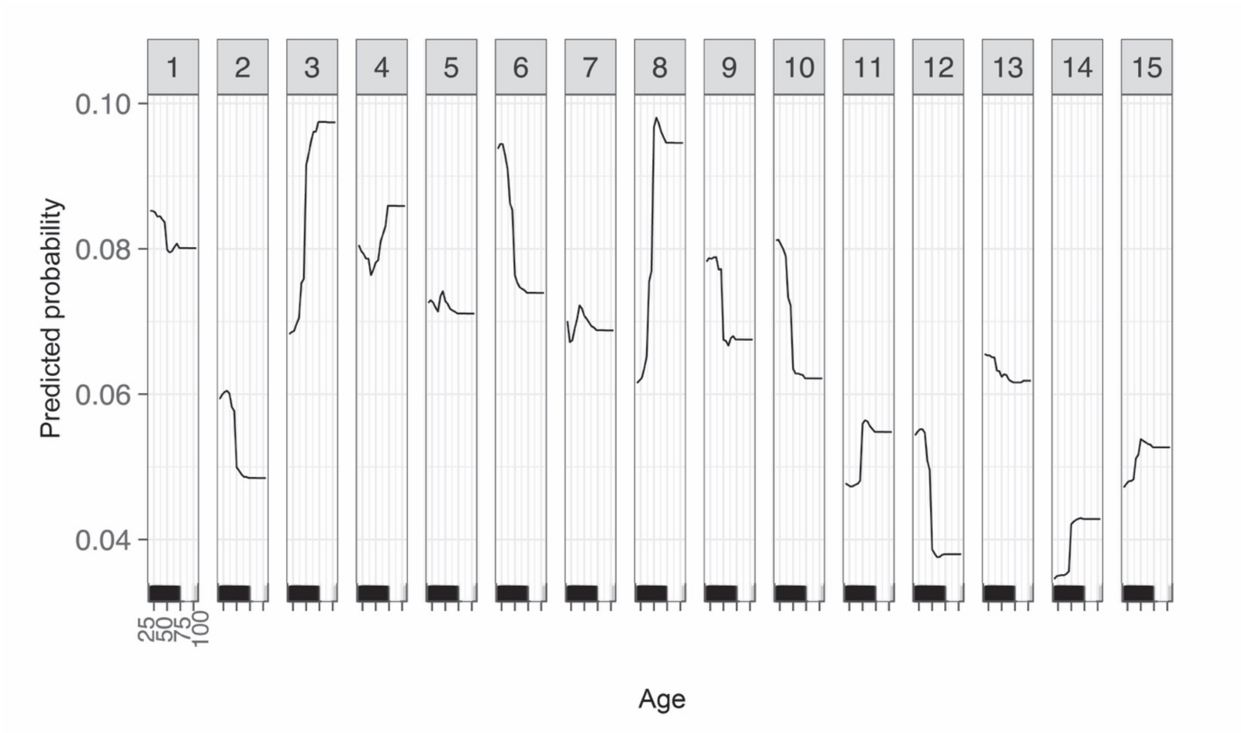

Supplementary Figure S12. Partial dependence plot for fifteen cluster solution. Probabilistic cluster membership across age. The y-axis is the probability of cluster membership. The black tick marks above the x-axis are data points such that the less tick marks the less participants at that level of the x-axis variable.

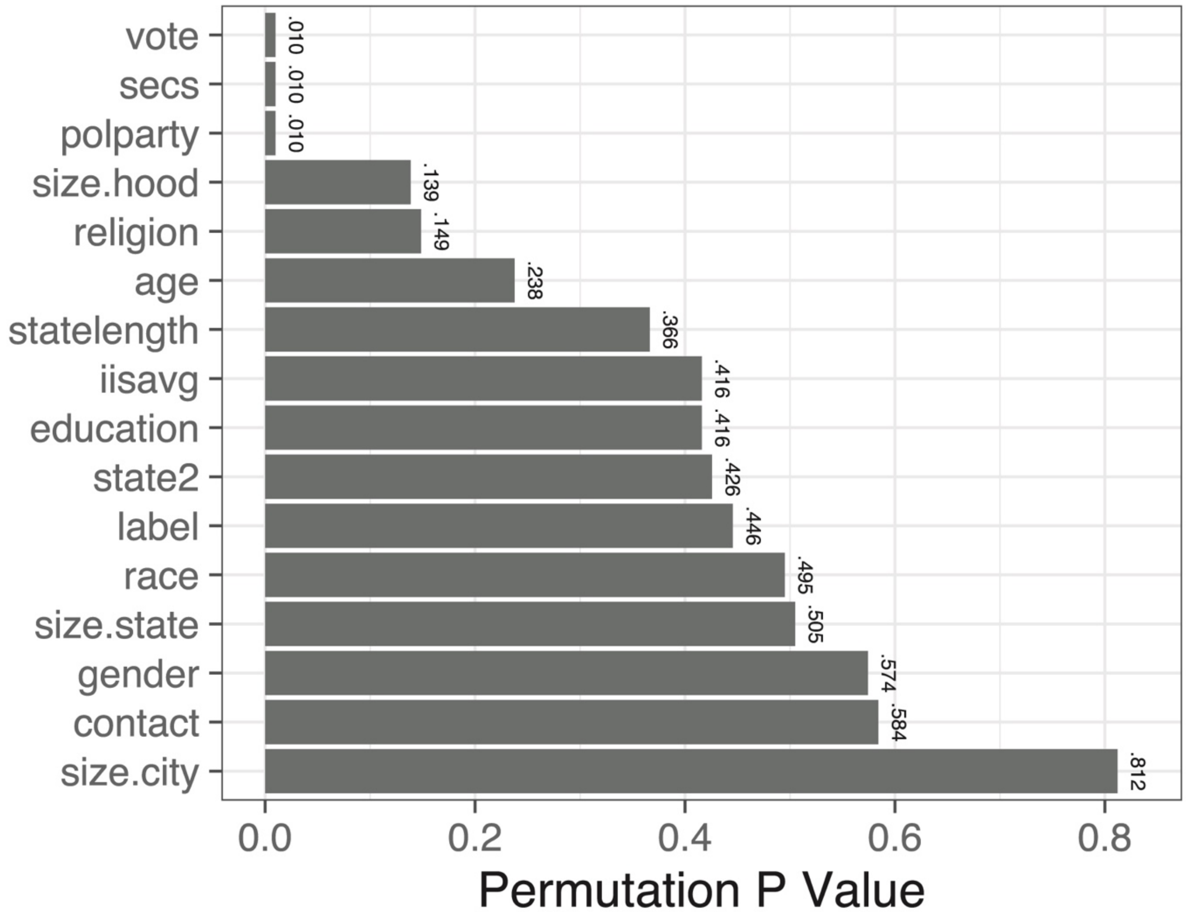

Supplementary Figure S13. Validation of random forest analysis and individual difference measures. As an initial step for validation, we calculated the variable importance for individual difference predictors of support for building the Mexico-U.S. wall. The x-axis is the permuted p value representing variable importance (significant alpha is .05). The exact p value is provided to the right of each bar. The y-axis lists all the individual difference measures. The results show that political variables (vote in 2016, social and economic conservatism, and political party affiliation) were the most important predictors of support for building the wall as could be expected given the politicized nature of Donald Trump's anti-immigrant proposal. **Supplementary Figure S14** shows how these three variables relate to support.

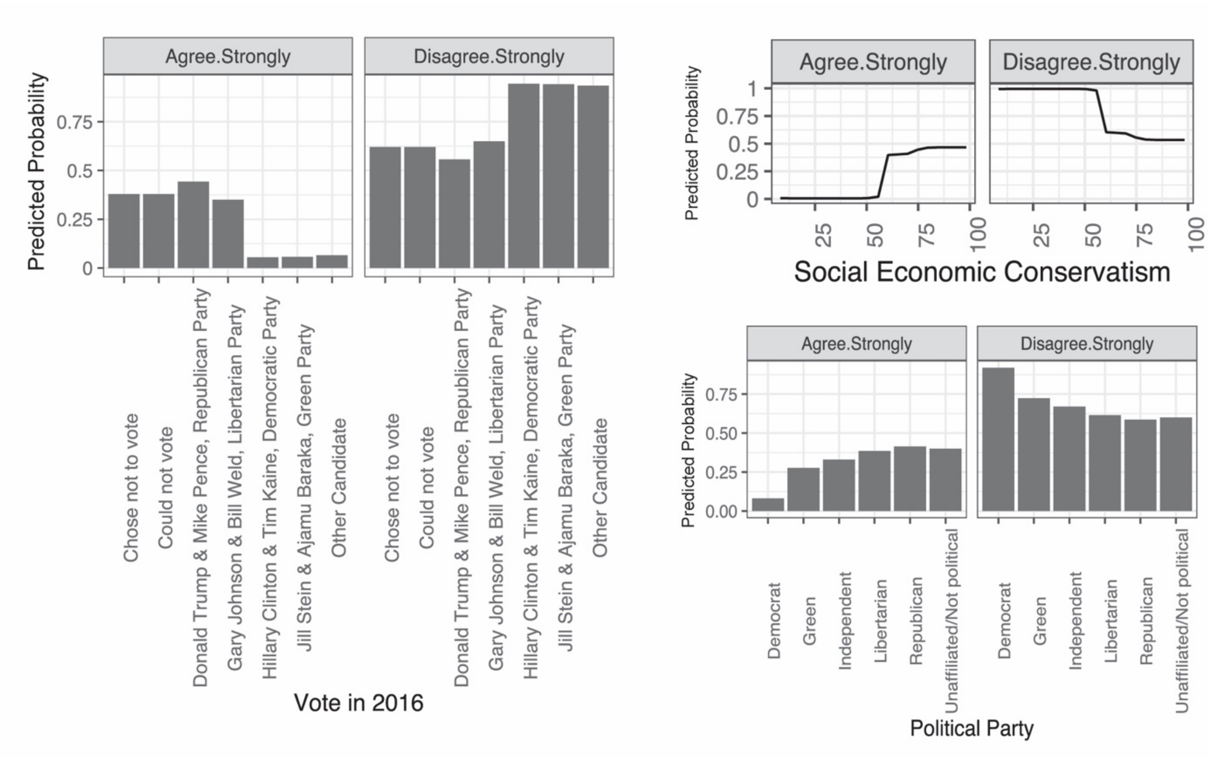

Supplementary Figure S14. Validation of random forest analysis and individual difference measures. Probabilistic responses of whether one agrees or disagrees strongly with building a Mexico-U.S. border wall across 2016 vote (top left panel), political orientation (top right panel), and political party (bottom right panel). The y-axis is the response probability. The x-axes are various presidential candidates (top left panel), political orientation scores (top right panel), and political parties (bottom right panel). For the 2016 vote, those who voted for more liberal or "other" candidates mostly disagreed strongly with building the wall. More conservative or libertarian voters and those who did not vote were more split in their support, yet overall were more likely to support, especially Donald Trump voters. For the social and economic conservatism scale, those who scored higher than 50 (i.e., more conservative) were split in their support, but overall were more likely to agree strongly than individuals who scored below 50 (i.e., more liberal). The more liberal respondents predominantly disagreed strongly. For political party affiliation, respondents from most of the party options were split in their support, except for Democrats who mainly disagreed strongly. Overall, there was less support for the wall, however, higher levels of support occurred for respondents from the Republican and Libertarian parties and who were unaffiliated. These patterns make theoretical sense and show that these techniques can capture meaningful relationships.